

COLORED VERTEX MODELS AND IWAHORI WHITTAKER FUNCTIONS

BEN BRUBAKER, VALENTIN BUCIUMAS, DANIEL BUMP, AND HENRIK P. A. GUSTAFSSON

ABSTRACT. We give a recursive method for computing all values of a basis of Iwahori Whittaker functions on a split reductive group G over a nonarchimedean local field F using an action of the Hecke algebra. Then we specialize to $G = \mathrm{GL}_r$ where we show that there exists a family of solvable lattice models whose partition functions give precisely these values. ‘Solvability’ of the model means there is a family of Yang-Baxter equations which imply, among other things, that these partition functions satisfy the same recursion as the Iwahori Whittaker functions. The R-matrices for these Yang-Baxter equations come from a Drinfeld twist of the quantum affine Lie superalgebra $U_q(\widehat{\mathfrak{gl}}(r|1))$, and are connected to the standard intertwining operators on the unramified principal series.

The lattice models we consider are similar to (but still different from) models introduced by Borodin and Wheeler. We explore relationships between our models and theirs, and between the partition functions and nonsymmetric Macdonald polynomials.

1. INTRODUCTION

One method of studying symmetric function theory and its generalizations is to represent polynomials as partition functions of solvable lattice models, as for example in [19, 30, 29, 43, 44, 25]. This introduces a powerful tool, the Yang-Baxter equation. More recently, the paper [10] considered families of solvable six-vertex models whose partition functions are values of Whittaker functions for the group $\mathrm{GL}_r(F)$ with F a nonarchimedean local field (or more generally a metaplectic covering group as in [9, 5, 7, 20]). Until now, these results have focused on *spherical* Whittaker functions, those invariant under a maximal compact subgroup. Yet it is very desirable to have lattice model representations for the larger class of Whittaker functions invariant under the Iwahori subgroup. A basis of these *Iwahori Whittaker functions* is indexed by elements of the associated Weyl group and they sum to the spherical Whittaker function. Even if one is mainly interested in the spherical Whittaker function, the Iwahori Whittaker functions play a key role in the theory ([15]).

A recent breakthrough by Borodin and Wheeler [3, 4] showed how to refine (generalizations of) the six-vertex model using an additional attribute they called ‘color.’ This led us to wonder whether there exists a similar refinement, applied to the (uncolored) model in [10], that might produce values of Iwahori Whittaker functions for the so-called standard basis. Remarkably the answer is affirmative, and its proof and implications are the subject of the present paper. Our results demonstrate that lattice models are unreasonably effective in modeling the representation theory of p -adic groups, and can serve as both a source of new results and a method for proving them.

We begin with a brief description of spherical Whittaker functions for $\mathrm{GL}_r(F)$ and their associated six-vertex models, which we will call *Tokuyama models*. Let \mathfrak{o} be the ring of integers of the nonarchimedean local field F and let v^{-1} be the cardinality of the residue field.

Form an unramified principal series representation of $\mathrm{GL}_r(F)$ from a character of $T(F)/T(\mathfrak{o})$ where T is the maximal split torus (see Section 2 for full details). These representations have unique Whittaker functionals and a unique-up-to-constant vector which is right invariant under $K = \mathrm{GL}_r(\mathfrak{o})$. The spherical Whittaker function is the image of this vector in the Whittaker functional and it is completely determined by its values on $T(F)/T(\mathfrak{o})$, which we identify with the weight lattice Λ of the Langlands dual group. It is easily seen that the spherical Whittaker function vanishes unless the associated weight is dominant. The remaining values for dominant weights are given by the Shintani-Casselman-Shalika formula in terms of Schur polynomials in the Langlands parameters of the principal series. By Tokuyama’s theorem, recalled below as Proposition 6.1 and described in [42, 10], there exists a family of solvable six-vertex models indexed by dominant weights whose partition functions give the Shintani-Casselman-Shalika formula.

There are multiple ways to describe the local conditions of the six-vertex model. We will primarily use two descriptions in this paper. First, we may decorate an edge in the model with a spin \pm so that each vertex in the model has adjacent edges in one of six possible configurations. The spins will be denoted by \oplus and \ominus both in the figures and in the rest of the text for readability. Alternately, we may use ‘line configurations’ as in Section 8.1 of [1], replacing each edge decoration \oplus or \ominus by the absence or presence of a path, respectively. Lattice models for GL_r will have r rows, and with the boundary conditions we will present, there will be exactly r paths in each admissible configuration beginning at the top boundary and traveling downward and rightward until each path exits on a distinct row along the right boundary. The lattice models are described in full detail in later sections of the paper, but the present snapshot will suffice to explain our results and methods.

As we noted above, Borodin and Wheeler [3] describe refinements of lattice models made with line configurations in which each path is assigned a color, and the colors decorating the starting and ending points of the paths become part of the boundary data defining the system of admissible configurations. In the six-vertex model, paths cross and so at each crossing there are multiple ways in which paths may be colored, resulting in multiple colored configurations for any one uncolored configuration (see for example Figure 20). The animating question of this paper then becomes: does there exist a set of weights for the colored model which simultaneously permit Yang-Baxter equations and so that the refined partition functions agree with values of Iwahori Whittaker functions — a family of functions fixed by the Iwahori subgroup J contained in the maximal compact K , thus refining the spherical Whittaker functions. In Section 4, we exhibit a set of colored Boltzmann weights and prove Yang-Baxter equations for them in Theorem 4.5. In Theorem 5.2 we use these Yang-Baxter equations to demonstrate that partition functions of colored systems are equal to values of Iwahori Whittaker functions in the standard basis.

We wish to highlight a particularly striking aspect of Theorem 5.2, which indicates how deeply the lattice model description is entwined with the p -adic representation theory. To explain it, we first need to describe some results from Section 2 valid for all split reductive groups G . Let $B = TN$ be a Borel subgroup with maximal split torus T and unipotent radical N . The Weyl group W , maximal compact subgroup K and a particular Iwahori subgroup J will be as defined in Section 2. We have a double coset decomposition $G = \sqcup_{w \in W} BwJ$ and therefore a basis ϕ_w of Iwahori Whittaker functions may be indexed by the Weyl group. Let $\Lambda = T(F)/T(\mathfrak{o})$, which we may think of as the weight lattice of the Langlands dual group. If

$\lambda \in \Lambda$ we will denote a representative in $T(F)/T(\mathfrak{o})$ as $\varpi^{-\lambda}$. Since $G = \cup_{w \in W, t \in T} NtwJ$, all values of all Iwahori Whittaker functions will be known if we can compute $\phi_{w_1}(\varpi^{-\lambda}w_2)$ for $w_1, w_2 \in W$ and $\lambda \in \Lambda$. One tends to focus on the case of λ dominant and $w_2 = 1$ because of their connection to spherical Whittaker functions; in the introduction to [38], Reeder notes that these values with $w_2 \neq 1$ are difficult to calculate. In Lemma 2.1, we give precise conditions on w_2 and the weight λ for the Whittaker value to be non-vanishing. *Then we may give a recursive method of computing the values $\phi_{w_1}(\varpi^{-\lambda}w_2)$ based on Propositions 2.2 and 2.4.*

Now returning to the results of Section 5 and the case $G = \text{GL}_r$, we find that our colored lattice models are perfectly suited to reflect each of the features of Whittaker functions described in the prior paragraph. In particular the admissible boundary conditions of our colored lattice models are in bijection with the pairs (λ, w_2) having nonzero Whittaker values at $\varpi^{-\lambda}w_2$ (Proposition 5.3) and the resulting partition function matches the value of the Whittaker function under this bijection in all cases (Theorem 5.2). The refinement from uncolored to colored models allows a richer set of boundary conditions which automatically detects this larger class of undetermined values of Iwahori Whittaker functions. That is, using the new results in Section 2, *we find that the partition functions that we obtain varying the boundary conditions compute exactly the $\phi_{w_1}(\varpi^{-\lambda}w_2)$ for all choices of w_1, w_2 and λ .*

We next describe relations between this work and earlier papers by the authors, emphasizing the known connections between their solvable models and modules for quantum groups. The *R-matrix* for the Yang-Baxter equation in the Tokuyama model is associated with the quantum affine Lie supergroup $U_{\sqrt{v}}(\widehat{\mathfrak{gl}}(1|1))$, as is shown in [5]. Alternatively, these ‘free-fermionic’ R-matrices can be related to a Drinfeld twist of $U_{\sqrt{-1}}(\widehat{\mathfrak{sl}}(2))$ ([34]), but in our view the generalizations discussed below show that it is better to rely on the superalgebra R-matrix.

The uniqueness of the spherical Whittaker function depends on two uniqueness results, as noted above. First, Whittaker models are unique for split reductive groups such as $\text{GL}_r(F)$; and second, in the principal series representation, there is a unique vector (up to normalization) that is fixed by the maximal compact subgroup K . In this paper, we relax the assumption that the vector is K -fixed in favor of Iwahori Whittaker functions, but we may also consider generalizing the group. If the ground field contains $2n$ distinct $2n$ -th roots of unity, we may replace the group $\text{GL}_r(F)$ by a (metaplectic) covering group $\widetilde{\text{GL}}_r^{(n)}$, and the Whittaker model is no longer unique. This produces n^r distinct Whittaker functionals.

We have described how the study of spherical Whittaker functions can be generalized to covering groups and Iwahori Whittaker functions, each choice breaking one of the local uniqueness statements. Let us now discuss how these generalizations may be achieved on the lattice model side by making modifications of the Tokuyama model. These connections are explained further in Sections 3 and 4. The various contexts are also summarized in Figure 1.

As mentioned above, the lattice for the Tokuyama six-vertex model is a grid made of horizontal and vertical edges, where each edge is assigned a ‘spin’ \oplus or \ominus . In [5] more general solvable lattice models were introduced representing metaplectic spherical Whittaker functions. In that theory, the spins of the horizontal edges are assigned an integer modulo n which we will call ‘charge’ that increases by 1 at each horizontal edge with spin \oplus . The edges with spin \ominus must have charge $\equiv 0$ modulo n . The vertical edges do not have charges, so there are $n + 1$ possible states (spin and charge) for the horizontal edges but only two for the vertical ones. The $n + 1$ possible states for the horizontal edges may be identified with

	GL_r no charges	$\widetilde{\mathrm{GL}}_r^{(n)}$ charges in $\mathbb{Z}/n\mathbb{Z}$
spherical, no colors	Tokuyama $U_{\sqrt{v}}(\widehat{\mathfrak{gl}}(1 1))$	Metaplectic ice [5] $U_{\sqrt{v}}(\widehat{\mathfrak{gl}}(1 n))$
Iwahori, r colors	This paper $U_{\sqrt{v}}(\widehat{\mathfrak{gl}}(r 1))$	Expected to be $U_{\sqrt{v}}(\widehat{\mathfrak{gl}}(r n))$

FIGURE 1. Summary of the different lattice models. For spherical Whittaker functions the models are not colored, while the models for Iwahori Whittaker functions have r different colors. When taking an n -fold cover, the horizontal states are assigned charges in $\mathbb{Z}/n\mathbb{Z}$.

basis vectors for an $(1|n)$ -dimensional super vector space. The R-matrix for the Yang-Baxter equation in these metaplectic models was identified with the Perk-Schultz [36, 45] R-matrix associated with the quantum affine supergroup $U_{\sqrt{v}}(\widehat{\mathfrak{gl}}(1|n))$.

Next consider the Iwahori models in this paper. We need r distinct colors to define the models. Only the \ominus spins are assigned a color, so the horizontal spins have $r + 1$ possible states, and we may think of them as the basis vectors of an $(r|1)$ -dimensional super vector space. In Section 4, we explain that the R-matrix for the Iwahori Whittaker functions is associated with the quantum supergroup $U_{\sqrt{v}}(\widehat{\mathfrak{gl}}(r|1))$.

The models in this paper have both similarities and differences from those in [5]. Whereas in [5] certain edges are enhanced by adding the charge attribute, in this paper we similarly enhance the system by decorating certain edges with color. Yet charges and colors are handled differently, and at first glance the schemes seem different. Nevertheless we will explain below how a different perspective shows that they are more similar than they first appear.

Before we can explain this point we have to introduce an equivalent form of the models. In these replace each vertex by r distinct *monochrome* vertices, and each vertical edge by r parallel *monochrome* edges. (See Figures 11 and 19.) For both the regular colored system and the monochrome version, the *horizontal* edges may carry any, but at most one color. On the other hand, for the colored systems, *vertical* edges may carry any and all colors, and indeed states exist in which an edge may carry two or more different colors (Figure 13). By contrast in the monochrome system, each *vertical* edge may carry at most one preassigned color; the edge has thus only two possible states, \oplus or its assigned color. The relationship between the colored models and their expanded monochrome models is described in Section 3. We will call this relationship *fusion*, as it is reminiscent of a similar fusion construction for quantum group modules (cf. [28] and Appendix B of [3]). See also [37].

Our fusion construction on monochrome vertices is the key to demonstrating the solvability of the colored models, paralleling the approach in [3]. In Section 3, we also comment on the relations between our fusion process and that of earlier work.

Furthermore, monochrome vertices lend a perspective that demonstrates another similarity between the models of this paper and the charged models in [5], as we now describe. In both the charged models of [5] and the colored models of this paper there is a relationship with

the uncolored states of the Tokuyama models. One may try to turn an uncolored state into an admissible state of metaplectic Gamma ice as in [5] by adding charges to the horizontal \oplus edges, and if it can be done it may be done so uniquely. So we may ask how to characterize the uncolored states that may be turned into states of metaplectic ice. This question has a simple answer: *it is necessary and sufficient that every contiguous sequence of \oplus horizontal edges (excepting those that reach the edge of the configuration) contain a multiple of n edges.*

By contrast, the problem of adding color to an uncolored state is trickier, as there may be more than one way to do it. Rather it is the expanded monochrome models that are most similar to metaplectic ice. For given a state of the uncolored system, if there is a way of adding color to obtain a state of the monochrome system, this way is unique. (See Section 6.) As in the metaplectic case, the characterization of such uncolored states is very simple: *it is necessary and sufficient that every contiguous sequence of \ominus horizontal edges (excepting those that reach the edge of the configuration) have a multiple of r edges.*

With this insight, it may be possible to consider the two devices of color and charge fundamentally equivalent, though at first they seem to be rather different schemes. It is possible to give colored systems whose partition functions are the same as those of the charged systems in [5], and vice versa. What is surprising is that one system gives spherical metaplectic Whittaker functions, and the other gives nonmetaplectic Iwahori Whittaker functions.

The two types of enhancements producing the metaplectic theory in [5] and the Iwahori theory in this paper are complementary, and it seems probable that one may give a model incorporating *both* charge and color representing the $n^r \cdot r!$ metaplectic Iwahori Whittaker functions. This idea is supported by the existence of metaplectic Demazure-Lusztig operators developed by Chinta, Gunnells, Patnaik and Puskás [35, 18]. It is natural to guess that the underlying quantum group will be $U_{\sqrt{v}}(\widehat{\mathfrak{gl}}(r|n))$.

In Sections 7 and 8, we explain relations between a subset of the partition functions of colored models in this paper and specializations of those of [3], including relations with nonsymmetric Macdonald polynomials. Such relations are interesting in light of the fact that the models in [3] are ‘bosonic’ (allowing multiplicities of colors on vertical edges), while those of the present paper are ‘fermionic’ (no multiplicities allowed).

Finally, in Section 9, we explain some further aspects of the “unreasonable effectiveness” of lattice models in studying p -adic representation theory. It is not just that the outputs of both lattice models and p -adic representation theory are the same, but that each tool or technique has an analog via this dictionary. Standard intertwining operators on principal series are a basic tool in the representation theory. Their action on Iwahori fixed vectors and how they interact with the Whittaker functional are the two principal ingredients in the Casselman-Shalika formula [14, 15] and are also the key to Proposition 2.4. Roughly, we show that these two actions of intertwining operators, on Iwahori fixed vectors and for the Whittaker functional, correspond to restrictions of the quantum superalgebra $U_{\sqrt{v}}(\widehat{\mathfrak{gl}}(r|1))$ to its $U_{\sqrt{v}}(\widehat{\mathfrak{gl}}(r))$ and $U_{\sqrt{v}}(\widehat{\mathfrak{gl}}(1))$ pieces, respectively.

More precisely, in Theorem 9.3 we show the action of the intertwining integral on the space of Iwahori fixed vectors is the same as the action of the affine R-matrix on a subspace of the tensor product of evaluation representations $V_r(z_1) \otimes \cdots \otimes V_r(z_r)$ of $U_{\sqrt{v}}(\widehat{\mathfrak{gl}}(r))$. This result is independent of the Whittaker functional and only the smaller quantum group $U_{\sqrt{v}}(\widehat{\mathfrak{gl}}(r)) \subset U_{\sqrt{v}}(\widehat{\mathfrak{gl}}(r|1))$ appears due to the fact that the right boundary conditions of

our model contain only colored edges (which span a subspace that can be thought of as the tensor product of evaluation representations of $U_{\sqrt{v}}(\widehat{\mathfrak{gl}}(r))$). The connection between Whittaker functionals and the scalar appearing in our restriction to $U_{\sqrt{v}}(\widehat{\mathfrak{gl}}(1))$ is explained in Remark 9.5.

A result similar to Theorem 9.3 was proved in the case of spherical Whittaker functions on the metaplectic n cover of GL_r in [5, Theorem 1.1], where the first three authors relate the Kazhdan-Patterson scattering matrix to the $U_{\sqrt{v}}(\widehat{\mathfrak{gl}}(n))$ R-matrix. The relation was used in [6] to build finite dimensional representations of the affine Hecke algebra starting from metaplectic Whittaker functionals. Theorem 9.3 now allows for a similar construction starting from Iwahori fixed vectors in an unramified principal series representation.

Acknowledgements: We thank Amol Aggarwal, Alexei Borodin, Siddhartha Sahi and Michael Wheeler for helpful conversations and communications. This work was supported by NSF grants DMS-1801527 (Brubaker) and DMS-1601026 (Bump), ARC grant DP180103150 (Buciumas) and the Knut and Alice Wallenberg Foundation (Gustafsson). Bump and Gustafsson also gratefully acknowledge the hospitality of the Simons Center for Geometry and Physics during parts of this project.

2. IWAHORI WHITTAKER FUNCTIONS

We will review the constructions of Iwahori Whittaker functions following [13]. There are several differences between choices made here and in [13] with those in Casselman-Shalika [15]. Let us summarize these choices, with notations to be defined more precisely below.

- As in [15], principal series representations are induced from the standard Borel subgroup B . But in contrast with [15], we will take Whittaker functions with respect to the unipotent radical N_- of the Borel subgroup B_- .
- We will take our Iwahori subgroup to be the preimage in the maximal compact subgroup K of B_- modulo \mathfrak{p} .
- We will apply our construction to the contragredient representation of the representation $\pi_{\mathbf{z}}$ with Langlands parameters \mathbf{z} .
- We will evaluate our Whittaker functions at values $\varpi^{-\lambda}$ of the maximal torus where $-\lambda$ is antidominant.

The advantage of these unconventional choices is that it keeps the long Weyl group element w_0 out of the formulas. Thus whereas for Casselman and Shalika the simplest Whittaker function is that supported on the double coset Bw_0J , and its value at ϖ^λ is (up to normalization), $\mathbf{z}^{w_0\lambda}$, with our conventions the simplest Whittaker function is supported on $B \cdot 1_W J$, and its value is (up to normalization) \mathbf{z}^λ .

In more detail, let F be a non-archimedean local field with ring of integers \mathfrak{o} . Let \mathfrak{p} be the maximal ideal of \mathfrak{o} with generator $\varpi \in \mathfrak{p}$. Then, ϖ is a prime element, or uniformizer, of F . We will denote by q the cardinality $q = |\mathfrak{o}/\mathfrak{p}|$ and the residue field itself by $\mathbb{F}_q = \mathfrak{o}/\mathfrak{p}$.

Let G be a split reductive Chevalley group, that is, an affine algebraic group scheme over \mathbb{Z} with a fixed Chevalley basis for its Lie algebra $\mathfrak{g}_{\mathbb{Z}}$. Let T be the standard maximal split torus of G obtained from our choice of Chevalley basis, and similarly let N be the standard maximal unipotent subgroup whose Lie algebra is the union of the positive root spaces. Together they form the standard Borel subgroup $B = TN$ and the Weyl group W is defined by $N_G(T)/T$ where $N_G(T)$ is the normalizer of T in G . For each Weyl group element w we

will always choose a representative in $K = G(\mathfrak{o})$ which is the maximal compact subgroup of $G(F)$. Let B_- be the opposite Borel subgroup and N_- be its unipotent radical generated by the negative root spaces. In the later sections of this paper we will mainly consider $G = \mathrm{GL}_r$ for which B is the subgroup of upper triangular matrices, T the diagonal matrices and B_- the lower triangular matrices.

Let \hat{G} be the Langlands dual group of G . We will denote the root system of \hat{G} by Δ and the simple roots of \hat{G} by $\alpha_1, \dots, \alpha_r$. The root system of G is the dual root system Δ^\vee . We prefer this notation instead of making Δ the root system of G , because the weight lattice Λ of \hat{G} appears frequently in the sequel.

We will consider an unramified character τ of $T(F)$, that is, a character that is trivial on $T(\mathfrak{o})$. The group of such characters is isomorphic to $\hat{T}(\mathbb{C}) \cong (\mathbb{C}^\times)^r$, where \hat{T} is the standard split maximal torus of \hat{G} . To define the unramified character $\tau_{\mathbf{z}}$ for $\mathbf{z} \in \hat{T}(\mathbb{C})$ we will use the following isomorphisms.

The group $X_*(T)$ of rational cocharacters of T is isomorphic to the weight lattice $\Lambda = X^*(\hat{T})$ of rational characters of the dual torus, and we will identify these two groups. But $X_*(T)$ is also isomorphic to the quotient $T(F)/T(\mathfrak{o})$. Indeed, if λ is a cocharacter let ϖ^λ be the image of the uniformizer ϖ in T under λ ; then we associate with λ the coset $\varpi^\lambda T(\mathfrak{o})$ in $T(F)/T(\mathfrak{o})$. On the other hand we may regard λ as a rational character and, with $\mathbf{z} \in \hat{T}$, let $\mathbf{z}^\lambda \in F^\times$ be the application of this character to \mathbf{z} . Then we define the unramified character $\tau_{\mathbf{z}}$ of $T(F)$ by $\tau_{\mathbf{z}}(t) = \mathbf{z}^\lambda$ when $t \in \varpi^\lambda T(\mathfrak{o})$.

In particular, for $G = \mathrm{GL}_r$ with $\lambda = (\lambda_1, \dots, \lambda_r) \in \mathbb{Z}^r \cong \Lambda$ and $\mathbf{z} = (z_1, \dots, z_r) \in (\mathbb{C}^\times)^r \cong \hat{T}(\mathbb{C})$ we let

$$\varpi^\lambda = \begin{pmatrix} \varpi^{\lambda_1} & & & \\ & \varpi^{\lambda_2} & & \\ & & \ddots & \\ & & & \varpi^{\lambda_r} \end{pmatrix} \in \mathrm{GL}_r(F) \text{ and } \tau_{\mathbf{z}}(\varpi^\lambda) = \mathbf{z}^\lambda = \prod_{i=1}^r z_i^{\lambda_i}.$$

The Iwahori subgroup J of $G(F)$ is the subgroup of $K = G(\mathfrak{o})$ defined as the preimage of $B_-(\mathbb{F}_q)$ under the mod \mathfrak{p} reduction map $K \rightarrow G(\mathbb{F}_q)$. For $G = \mathrm{GL}_r$ the Iwahori subgroup consists of elements in $\mathrm{GL}_r(\mathfrak{o})$ which are lower triangular mod \mathfrak{p} .

We trivially extend an unramified character $\tau_{\mathbf{z}}$ of $T(F)$ to $B(F)$ and let $(\pi, I(\mathbf{z}))$ denote the induced representation $I(\mathbf{z}) = \mathrm{Ind}_B^G(\delta^{1/2}\tau_{\mathbf{z}})$ under the right-regular action π of $G(F)$ where $\delta : B(F) \rightarrow \mathbb{R}^\times$ is the modular quasicharacter.

Consider the space $I(\mathbf{z})^J$ of Iwahori fixed vectors in $I(\mathbf{z})$ which is of dimension $\dim I(\mathbf{z})^J = |W|$. We will now describe a basis for $I(\mathbf{z})^J$ which will be used throughout the paper. By combining the Bruhat decomposition $G(F) = \bigsqcup_{w \in W} B(F)wB(F)$ and the Iwahori factorization $J = N(\mathfrak{p})T(\mathfrak{o})N_-(\mathfrak{o})$ one can show that $G = \bigsqcup_{w \in W} B(F)wJ$ [14]. Then, the elements $\Phi_w^{\mathbf{z}} \in I(\mathbf{z})^J$ for $w \in W$ defined by

$$\Phi_w^{\mathbf{z}}(bw'k) := \begin{cases} \delta^{1/2}\tau_{\mathbf{z}}(b) & \text{if } w' = w \\ 0 & \text{otherwise} \end{cases} \quad b \in B(F), w' \in W, k \in J$$

form a basis of $I(\mathbf{z})^J$, commonly referred to as the ‘standard basis.’

For $\alpha \in \Delta$, let $x_\alpha : \mathbb{G}_a \rightarrow G$ be the one-parameter subgroup of G tangent to the coroot α^\vee , which is a root of G because Δ is the root system of the dual group \hat{G} . Fix a unitary

character ψ on $N_-(F)$ such that, for any α^\vee , $\psi \circ x_\alpha : F \rightarrow \mathbb{C}^\times$, is a character on F trivial on \mathfrak{o} but no larger fractional ideal. The space of Whittaker functionals, which are linear maps $\Omega_{\mathbf{z}} : I(\mathbf{z}) \rightarrow \mathbb{C}$ satisfying $\Omega_{\mathbf{z}}(\pi(n_-)f) = \psi(n_-)\Omega_{\mathbf{z}}(f)$ for $n_- \in N_-(F)$, is one dimensional [39]. We need therefore only consider the following explicit Whittaker functional

$$(1) \quad \Omega_{\mathbf{z}}(f) := \int_{N_-(F)} f(n)\psi(n)^{-1} dn \quad f \in I(\mathbf{z}).$$

The integral is convergent if $|\mathbf{z}^\alpha| < 1$ for positive roots α , and can be extended to all \mathbf{z} by analytic continuation.

The objects of study in this paper are the *Iwahori Whittaker functions* obtained by applying the Whittaker functional (1) to right-translates of standard basis elements $\Phi_w^{\mathbf{z}}$. According to the left $N_-(F)$ equivariance and the right J invariance, these functions are determined by their values at $\varpi^\lambda w$ with $\varpi^\lambda \in T(F)/T(\mathfrak{o})$ and $w \in W$. To simplify the notation for these functions in the later sections, we will use the following conventions and normalizations for Whittaker functions of the contragredient $I(\mathbf{z}^{-1})$ of $I(\mathbf{z})$ at these values. For a weight $\lambda \in \Lambda$ and $w_1, w_2 \in W$, we consider the Iwahori Whittaker function

$$(2) \quad \phi_{w_1}(\mathbf{z}; \varpi^{-\lambda}w_2) := \delta^{-1/2}(\varpi^\lambda)\Omega_{\mathbf{z}^{-1}}\left(\pi(\varpi^{-\lambda}w_2)\Phi_{w_1}^{\mathbf{z}^{-1}}\right).$$

In [13] the notation $\mathcal{W}_{\lambda, w_1}(\mathbf{z})$ was used instead, but with the Whittaker function evaluated only at torus elements $\varpi^{-\lambda}$. In this paper we treat the general case, not only $w_2 = 1$, and will therefore need the notation $\phi_{w_1}(\mathbf{z}; \varpi^{-\lambda}w_2)$.

We say that λ is *w-almost dominant* if for all simple roots α_i

$$(3) \quad \begin{cases} \langle \alpha_i^\vee, \lambda \rangle \geq 0 & \text{if } w^{-1}\alpha_i \in \Delta^+, \\ \langle \alpha_i^\vee, \lambda \rangle \geq -1 & \text{if } w^{-1}\alpha_i \in \Delta^-, \end{cases}$$

and the following lemma shows how this is related to the non-vanishing of $\phi_{w_1}(\mathbf{z}; \varpi^{-\lambda}w_2)$.

Lemma 2.1. *Let \mathcal{W} be a J -invariant Whittaker function. Then*

$$\mathcal{W}(\varpi^{-\lambda}w_2) = 0$$

unless λ is w_2 -almost dominant.

Proof. This is similar to Lemma 5.1 of [15]. Let α_i be a simple root such that (3) fails. We may find $t \in \mathfrak{p}^{-1}$ such that $\psi(u) \neq 1$ where $u = x_{-\alpha_i}(t)$. Now

$$\psi(u)\mathcal{W}(\varpi^{-\lambda}w_2) = \mathcal{W}(u\varpi^{-\lambda}w_2) = \mathcal{W}(\varpi^{-\lambda}w_2j)$$

where

$$j = w_2^{-1}\varpi^\lambda u \varpi^{-\lambda}w_2 = x_{-w_2(\alpha_i)}(\varpi^{-\langle \alpha_i^\vee, \lambda \rangle}t).$$

Our assumption that (3) fails implies that $\varpi^{-\langle \alpha_i^\vee, \lambda \rangle}t \in \mathfrak{o}$ if $w_2(\alpha) \in \Delta^+$ and $\varpi^{-\langle \alpha_i^\vee, \lambda \rangle}t \in \mathfrak{p}$ if $w_2(\alpha) \in \Delta^-$ and in either case $j \in J$, so $\mathcal{W}(\varpi^{-\lambda}w_2j)$ equals $\mathcal{W}(\varpi^{-\lambda}w_2)$ which must therefore vanish. \square

Next we analyze the special case $w_1 = w_2$. To any $w \in W$, let Δ_w^+ denote the set of positive roots $\{\alpha \in \Delta^+ \mid w(\alpha) \in \Delta^-\}$.

Proposition 2.2. *Let $w \in W$ and $\lambda \in \Lambda$ a w -almost dominant weight. Then*

$$\phi_w(\mathbf{z}; \varpi^{-\lambda}w) = q^{-\ell(w)}\mathbf{z}^\lambda,$$

where $\ell(w)$ denotes the length of a reduced expression for w .

Proof. By definition

$$\phi_w(\mathbf{z}; \varpi^{-\lambda}w) = \delta^{-1/2}(\varpi^\lambda) \int_{N_-(F)} \Phi_w^{\mathbf{z}^{-1}}(n\varpi^{-\lambda}w)\psi(n)^{-1}dn.$$

We make the variable change $n \mapsto \varpi^{-\lambda}n\varpi^\lambda$. This multiplies the measure by $\delta(\varpi^\lambda)$ and using $\Phi_w^{\mathbf{z}^{-1}}(\varpi^{-\lambda}g) = \delta^{1/2}(\varpi^{-\lambda})\mathbf{z}^\lambda\Phi_w^{\mathbf{z}^{-1}}(g)$ we get

$$\mathbf{z}^\lambda \int_{N_-(F)} \Phi_w^{\mathbf{z}^{-1}}(nw)\psi(\varpi^{-\lambda}n\varpi^\lambda)^{-1}dn.$$

Let $J_w = wJw^{-1}$. This has the Iwahori factorization $J_w = N_w^-T(\mathfrak{o})N_w^+$ where $N_w^- = J_w \cap N_-(F)$ and similarly for N_w^+ . In particular

$$(4) \quad N_w^- = \prod_{\alpha \in \Delta^+} \begin{cases} x_{-\alpha}(\mathfrak{o}) & \text{if } w^{-1}\alpha \in \Delta^+, \\ x_{-\alpha}(\mathfrak{p}) & \text{if } w^{-1}\alpha \in \Delta^-. \end{cases}$$

The integrand is nonzero only if $nw \in BwJ$. We will show that this is true if and only if $n \in N_w^-$. Indeed, write $nw = bwj$ where $j \in J$. Then $n = bj_w$ where $j_w = wjw^{-1} \in J_w$. Using the Iwahori factorization, $j_w = \beta n_w^-$ where $\beta \in B$ and $n_w^- \in N_w^-$. Because $B \cap N_- = 1$, $b = \beta = 1$ and $n = n_w^-$. Therefore the integral equals

$$\mathbf{z}^\lambda \int_{N_w^-} \Phi_w^{\mathbf{z}^{-1}}(nw)\psi(\varpi^{-\lambda}n\varpi^\lambda)^{-1}dn.$$

Now we will show that the value of the integrand is 1 so this is just \mathbf{z}^λ times the volume of N_w^- . We have $\Phi_w^{\mathbf{z}^{-1}}(nw) = 1$ since the argument is in wJ . We must show that $\varpi^{-\lambda}n\varpi^\lambda$ is in the kernel of ψ . For this it is sufficient to show that if $\alpha = \alpha_i$ is a simple positive root then

$$\varpi^{-\lambda}x_{-\alpha_i}(t)\varpi^\lambda \in N_-(\mathfrak{o})$$

where using (4) we may assume that $t \in \mathfrak{o}$ if $w^{-1}(\alpha_i) \in \Delta^+$ and $t \in \mathfrak{p}$ otherwise. Now

$$\varpi^{-\lambda}x_{-\alpha_i}(t)\varpi^\lambda = x_{-\alpha_i}(\varpi^{\langle \lambda, \alpha_i^\vee \rangle}t).$$

Because λ is w -almost dominant $\varpi^{\langle \lambda, \alpha_i^\vee \rangle}t$ is indeed in \mathfrak{o} .

Hence $\phi_w(\mathbf{z}; \varpi^{-\lambda}w)$ equals \mathbf{z}^λ times the volume of N_w^- , which is $q^{-\ell(w)}$. \square

In order to determine the values of the Iwahori Whittaker function $\phi_{w_1}(\mathbf{z}; \varpi^{-\lambda}w_2)$ in full generality, we mimic the methods of [13], which used ingredients from earlier papers of Casselman and Shalika [14, 15]. In brief, we will develop a recursion using the Bruhat order in the Weyl group in the w_1 variable above, whose base case is given by Proposition 2.2. The recursion results from computing the function $\Omega_{\mathbf{z}}(\mathcal{A}_{s_i} \cdot \Phi_w)$ in two ways, where \mathcal{A}_w denotes the standard intertwining operator on principal series corresponding to the Weyl group element $w \in W$ and s_i is a simple reflection. Comparing the two methods of computation will give the values of the Whittaker function. We begin by briefly reviewing the basics of intertwining operators. These facts will also be needed in Section 9.

The standard intertwining integral $\mathcal{A}_w^{\mathbf{z}} : I(\mathbf{z}) \rightarrow I(w\mathbf{z})$ is given by

$$\mathcal{A}_w^{\mathbf{z}}\Phi(g) = \int_{N(F) \cap wN_-(F)w^{-1}} \Phi(w^{-1}ng)dn.$$

The integral converges when $|\mathbf{z}^\alpha| < 1$ for $\alpha \in \Delta^+$ and can be extended to arbitrary \mathbf{z} by meromorphic continuation. The intertwining integral induces a map $\mathcal{A}_w^{\mathbf{z}} : I(\mathbf{z})^J \rightarrow I(w\mathbf{z})^J$

and an explicit expression for $\mathcal{A}_{s_i}^{\mathbf{z}}$ on $I(\mathbf{z})^J$ is given by the following formula. See Proposition 3 in [13] for a proof of this fact, which is equivalent to Theorem 3.4 of [14]:

$$(5) \quad \mathcal{A}_{s_i}^{\mathbf{z}}(\Phi_w^{\mathbf{z}}) = \begin{cases} (1 - c_{\alpha_i}(s_i\mathbf{z}))\Phi_w^{s_i\mathbf{z}} + \Phi_{s_i w}^{s_i\mathbf{z}} & \text{if } \ell(s_i w) > \ell(w), \\ (q^{-1} - c_{\alpha_i}(s_i\mathbf{z}))\Phi_w^{s_i\mathbf{z}} + q^{-1}\Phi_{s_i w}^{s_i\mathbf{z}} & \text{if } \ell(s_i w) < \ell(w), \end{cases}$$

where

$$(6) \quad c_{\alpha_i}(\mathbf{z}) = \frac{1 - q^{-1}\mathbf{z}^{\alpha_i}}{1 - \mathbf{z}^{\alpha_i}}.$$

Substituting in the definition of c_{α_i} and using that $(s_i\mathbf{z})^{\alpha_i} = \mathbf{z}^{-\alpha_i}$ we get that equation (5) is equivalent to

$$(7) \quad (1 - \mathbf{z}^{\alpha_i})\mathcal{A}_{s_i}^{\mathbf{z}}(\Phi_w^{\mathbf{z}}) = \begin{cases} (1 - q^{-1})\Phi_w^{s_i\mathbf{z}} + (1 - \mathbf{z}^{\alpha_i})\Phi_{s_i w}^{s_i\mathbf{z}} & \text{if } \ell(s_i w) > \ell(w), \\ \mathbf{z}^{\alpha_i}(1 - q^{-1})\Phi_w^{s_i\mathbf{z}} + q^{-1}(1 - \mathbf{z}^{\alpha_i})\Phi_{s_i w}^{s_i\mathbf{z}} & \text{if } \ell(s_i w) < \ell(w). \end{cases}$$

In Proposition 2 of [13], following from Proposition 4.3 of [15], the following result is proven.

Proposition 2.3. *For any $w \in W$,*

$$\Omega_{w\mathbf{z}} \circ \mathcal{A}_w^{\mathbf{z}} = \left(\prod_{\alpha \in \Delta_w^+} \frac{1 - q^{-1}\mathbf{z}^{-\alpha}}{1 - \mathbf{z}^{-\alpha}} \right) \Omega_{\mathbf{z}}.$$

In Proposition 2.4 below we will combine the above results to obtain a recursion relation for $\phi_w(\mathbf{z}; g)$ using Demazure type operators that we will define now.

Let \mathcal{O} be the ring of regular (polynomial) functions on $\hat{T} = (\mathbb{C}^\times)^r$. This ring is isomorphic to the group algebra of $\Lambda = \mathbb{Z}^r$ as follows. If $\mathbf{z} = (z_1, \dots, z_r) \in \hat{T}$ and $\lambda \in \Lambda$ let $\mathbf{z}^\lambda = \prod z_i^{\lambda_i}$. Then \mathcal{O} is spanned by the functions \mathbf{z}^λ . We may now define some operators \mathfrak{T}_i on \mathcal{O} as follows. Let v be a nonzero complex number and, for $f \in \mathcal{O}$, let

$$(8) \quad \mathfrak{T}_{i,v}f(\mathbf{z}) = \mathfrak{T}_i f(\mathbf{z}) = \frac{f(\mathbf{z}) - f(s_i\mathbf{z})}{\mathbf{z}^{\alpha_i} - 1} - v \frac{f(\mathbf{z}) - \mathbf{z}^{-\alpha_i}f(s_i\mathbf{z})}{\mathbf{z}^{\alpha_i} - 1}.$$

These operators satisfy the braid relations (see for example Proposition 5 of [13]):

$$\mathfrak{T}_i \mathfrak{T}_{i+1} \mathfrak{T}_i = \mathfrak{T}_{i+1} \mathfrak{T}_i \mathfrak{T}_{i+1},$$

while \mathfrak{T}_i and \mathfrak{T}_j commute if $|i - j| > 1$. They also satisfy the quadratic relation

$$\mathfrak{T}_i^2 = (v - 1)\mathfrak{T}_i + v.$$

This quadratic relation implies that \mathfrak{T}_i is invertible. Indeed its inverse is

$$(9) \quad \mathfrak{T}_i^{-1}f(\mathbf{z}) = \frac{\mathbf{z}^{-\alpha_i}f(s_i\mathbf{z}) - \mathbf{z}^{\alpha_i}f(\mathbf{z})}{\mathbf{z}^{\alpha_i} - 1} - \frac{f(s_i\mathbf{z}) - \mathbf{z}^{\alpha_i}f(\mathbf{z})}{v(\mathbf{z}^{\alpha_i} - 1)}.$$

See [13] Propositions 5 and 6 for proofs of these facts.¹ The operators \mathfrak{T}_i thus generate a finite Iwahori Hecke algebra. They are similar to the well-known *Demazure-Lusztig operators*, which by comparison send f to

$$(10) \quad \mathfrak{L}_{i,v}f(\mathbf{z}) = \mathfrak{L}_i f(\mathbf{z}) = \frac{f(\mathbf{z}) - f(s_i\mathbf{z})}{\mathbf{z}^{\alpha_i} - 1} - v \frac{f(\mathbf{z}) - \mathbf{z}^{\alpha_i}f(s_i\mathbf{z})}{\mathbf{z}^{\alpha_i} - 1}.$$

¹All references to [13] are to the published version; the operators in the arXiv version are slightly different.

As we will discuss in Section 8, the difference is slight but significant. We will refer to the \mathfrak{T}_i operators in (8) as *Demazure-Whittaker operators*.

The following result generalizes Theorem 2 of [13].

Proposition 2.4. *For any $w \in W$, a simple reflection s_i , and with $v = q^{-1}$,*

$$(11) \quad \phi_{s_i w}(\mathbf{z}; g) = \begin{cases} \mathfrak{T}_i \cdot \phi_w(\mathbf{z}; g) & \text{if } \ell(s_i w) > \ell(w), \\ \mathfrak{T}_i^{-1} \cdot \phi_w(\mathbf{z}; g) & \text{if } \ell(s_i w) < \ell(w), \end{cases}$$

where the \mathfrak{T}_i and their inverses are as in (8) and (9).

Proof. The result follows from combining the relation (7) with Proposition 2.3, recalling from (2) that the Whittaker functions $\phi_w(\mathbf{z}; g)$ are made with respect to principal series with the Langlands parameter \mathbf{z}^{-1} . \square

Proposition 2.4 gives a recursion on Iwahori fixed vectors ϕ_w which is independent of the word used to represent w .

Corollary 2.5. *Given any w_1, w_2 and a w_2 -almost dominant weight λ , let $(s_{i_1}, \dots, s_{i_k})$ be any path in the Bruhat order from w_2 to w_1 (so $w_2 \rightarrow s_{i_1} w_2 \rightarrow \dots \rightarrow s_{i_k} \dots s_{i_1} w_2 = w_1$). Set e_{i_j} to be +1 or -1 depending on whether s_{i_j} is a descent or ascent, respectively, in Bruhat order. Then, with $v = q^{-1}$,*

$$\phi_{w_1}(\mathbf{z}; \varpi^{-\lambda} w_2) = v^{\ell(w_2)} \mathfrak{T}_{i_k}^{e_{i_k}} \dots \mathfrak{T}_{i_1}^{e_{i_1}} \mathbf{z}^\lambda.$$

Proof. This corollary follows immediately from Propositions 2.2 and 2.4. It generalizes Theorem 1 of [13], which evaluates the special case $w_2 = 1$. \square

Corollary 2.6. *Suppose that $w_2 \leq w_1$ in the Bruhat order. Then*

$$(12) \quad \phi_{w_1}(z; \varpi^{-\lambda} w_2) = v^{\ell(w_2)} \phi_{w_1 w_2^{-1}}(z; \varpi^{-\lambda}).$$

Proof. Taking a reduced expression $s_{i_1} \dots s_{i_k}$ for $w_1 w_2^{-1}$, by Corollary 2.5 both sides equal

$$v^{\ell(w_2)} \mathfrak{T}_{i_1} \dots \mathfrak{T}_{i_k} \mathbf{z}^\lambda.$$

\square

3. LATTICE MODELS, YANG-BAXTER EQUATIONS AND FUSION

The models that we will be concerned with take place on planar graphs. In using the term *graph* to describe these arrays we are deviating from usual terminology, where edges have always two vertices, for we will allow open edges with only a single endpoint. Thus we mean a set of *vertices* which are points in the plane, together with *edges* that are arcs which either join two vertices, or which are attached to only a single vertex. The edges which are only attached to a single vertex are called *boundary edges*. The edges attached to two vertices are called *interior edges*. Every vertex is adjacent to four edges. Edges can only cross at a vertex.

For every edge A in the model there is an allowed set Σ_A of states called *spins*.

Assumption 3.1. *At each vertex, let A, B, C, D be the four adjacent edges, arranged so that A and C are opposite edges, as are B and D . Then $\Sigma_A = \Sigma_C$ and $\Sigma_B = \Sigma_D$.*

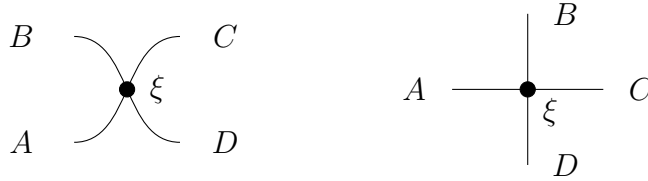


FIGURE 2. Left: a vertex adjoining four horizontal edges. Such a vertex will be called an *R-vertex*. Right: A vertex adjoining two horizontal edges and two vertical ones. We will call such vertices *ordinary*. Each vertex receives a label ξ corresponding to its Boltzmann weights.

Each vertex has a label ξ , and an associated set of *Boltzmann weights* β_ξ . This is a rule which assigns a complex number to every possible choice of spins at the four adjacent edges of the vertex. Thus if A, B, C, D are the four adjacent edges to a vertex with label ξ , this data consists of a map

$$\beta_\xi : \Sigma_A \times \Sigma_B \times \Sigma_C \times \Sigma_D \rightarrow \mathbb{C}.$$

We call the set of spins $(a, b, c, d) \in \Sigma_A \times \Sigma_B \times \Sigma_C \times \Sigma_D$ a *configuration* at the vertex. The configuration is *admissible* if $\beta_\xi(a, b, c, d) \neq 0$.

Assumption 3.2. *At each vertex, if three out of four spins in (a, b, c, d) in an admissible configuration are given, the fourth is uniquely determined.*

In a system \mathfrak{S} , the data specifying the system are the graph itself, the spin sets Σ_A and the Boltzmann weight data β_ξ for each label ξ . For example, the labels ξ might be complex numbers and β_ξ are uniformly described as a set of complex-valued functions of ξ for each configuration. Moreover the spins of the boundary edges are fixed, and are part of the data specifying the system.

A *state* \mathfrak{s} of the system is an assignment of spins to the interior edges. That is, for each edge A there is specified a spin $\mathfrak{s}_A \in \Sigma_A$. We will use the notation $\mathfrak{s} \in \mathfrak{S}$ to mean that \mathfrak{s} is a state of the system. The *Boltzmann weight* $\beta(\mathfrak{s})$ of the state is the product of the Boltzmann weights at the labelled vertices and the state is said to be *admissible* if all of its vertices are admissible. The *partition function* $Z(\mathfrak{S})$ is the sum of the Boltzmann weights of all the (admissible) states.

In the systems that we will consider, the edges all may be classified as either *horizontal* or *vertical*. There will be two types of vertices. In one type, the vertex intersects four horizontal edges and will be called an *R-vertex*. In the other, called *ordinary*, it intersects two horizontal and two vertical ones. See Figure 2.

Next we explain a procedure we refer to as *fusion* for producing new kinds of edges and vertices from given ones. (This is partly inspired by a process of the same name described in Borodin and Wheeler [3], Appendix B.)

Given a sequence of edges, A_1, \dots, A_m we may replace these with a single edge \mathbf{A} such that $\Sigma_{\mathbf{A}} = \prod_k \Sigma_{A_k}$. This edge is called the *fusion* of the edges $\{A_k\}$. Next assume that we have a sequence of m *ordinary* vertices with labels ξ_1, \dots, ξ_m such that the vertex with label ξ_k is adjoined to the vertex with label ξ_{k+1} by an edge E_k if $1 \leq k \leq m-1$. Let the remaining adjacent edges of the vertex with label ξ_k be B_k and D_k and A (if $k=1$) and C if $k=m$. Thus the configuration is as in Figure 3 (left).

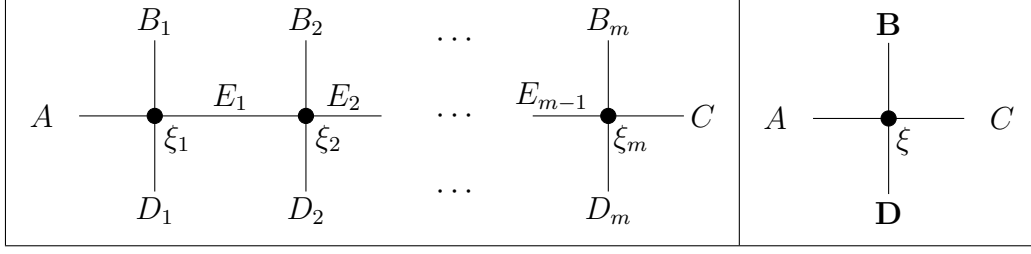


FIGURE 3. Fusion. This procedure replaces a sequence of vertices by a single vertex.

Now we may construct the fusion \mathbf{B} of the edges B_i as above, as well as the fusion \mathbf{D} of the edges D_i . We may then fuse the vertices, replacing the sequence of m vertices with labels ξ_1, \dots, ξ_m by a single vertex labeled ξ (as in Figure 3). It remains to discuss the Boltzmann weights. Let spins $(a, b, c, d) \in \Sigma_A \times \Sigma_{\mathbf{B}} \times \Sigma_C \times \Sigma_{\mathbf{D}}$. By definition b and d are sequences of spins $b_k \in \Sigma_{B_k}$ and $d_k \in \Sigma_{D_k}$. Fixing (a, b, c, d) , it follows from Assumption 3.2 that the system in Figure 3 (left) has at most one (admissible) state. We define $\beta_\xi(a, b, c, d)$ to be its partition function. It is clear that Assumption 3.2 remains valid for this fused vertex.

At any vertex, it will be useful to choose a clockwise ordering (A, B, C, D) of the adjoining edges. In our illustrations, we will always choose the ordering as in Figure 2. If A is an edge, we will denote by V_A the free vector space with basis Σ_A . By Assumption 3.1, we may identify $V_A = V_C$ and $V_B = V_D$. Then the Boltzmann weights at a vertex with label ξ define an element of $\text{End}(V_A \otimes V_B)$ by

$$(13) \quad a \otimes b \mapsto \sum_{(c,d) \in \Sigma_C \times \Sigma_D} \beta_\xi(a, b, c, d)(c \otimes d).$$

If the vertex is an R-vertex we will denote this endomorphism as R_ξ ; this endomorphism is called an *R-matrix*. For ordinary vertices, we will denote the endomorphism (13), which is called a *transfer matrix*, as T_ξ .

Definition 3.3. Suppose that, for ordinary vertices labeled ξ, η and R-vertex labeled ζ , there exists Boltzmann weights such that for every choice of boundary spins (a, b, c, d, e, f) the partition functions of the two systems in Figure 4 are equal. Then we say we have a solution of the *Yang-Baxter equation*.

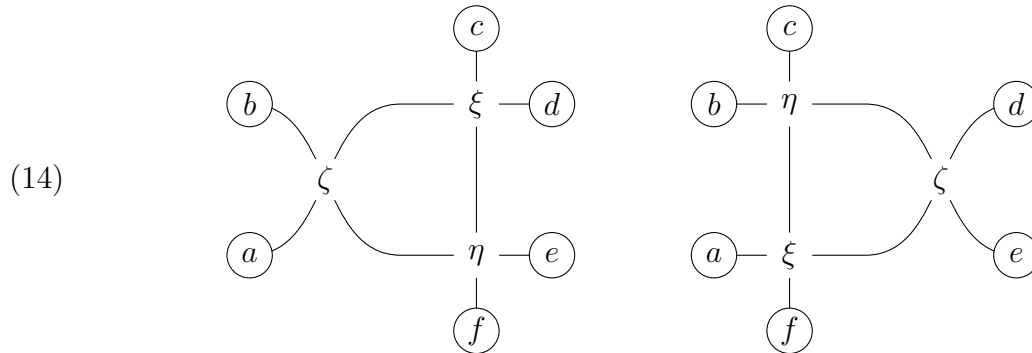


FIGURE 4. The Yang-Baxter equation.

Let A, B, C, D, E, F be the boundary edges of these configurations, so that $a \in \Sigma_A$, etc. By Assumption 3.1 $V_A = V_D, V_B = V_E$ and $V_C = V_F$. Then $R_\zeta \in \text{End}(V_A \otimes V_B)$, $T_\xi \in \text{End}(V_A \otimes V_C)$ and $T_\eta \in \text{End}(V_B \otimes V_C)$. The Yang-Baxter equation can be expressed in the formula

$$(15) \quad (R_\zeta)_{12}(T_\xi)_{13}(T_\eta)_{23} = (T_\eta)_{23}(T_\xi)_{13}(R_\zeta)_{12},$$

an identity in $\text{End}(V_A \otimes V_B \otimes V_C)$, where, in the notation common in quantum group theory, $(R_\zeta)_{12}$ denotes R_ζ acting on the first two components of $V_A \otimes V_B \otimes V_C$ and so forth. We wish to consider examples of (14) where the ordinary vertices arise from the fusion process described above. Thus the left configuration can be expanded as in Figure 5.

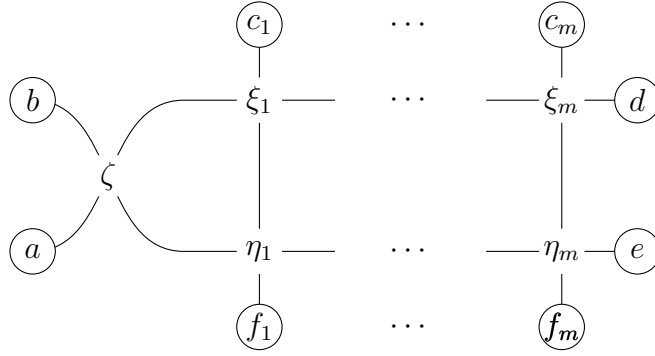


FIGURE 5. Setup for the Yang-Baxter equation with fused vertices ξ and η .

Lemma 3.4. *Suppose there exists a sequence of R -vertices with labels $\zeta_1, \dots, \zeta_{m+1}$ such that $\zeta_1 = \zeta_{m+1} = \zeta$ and such that for each $1 \leq k \leq m$, the two partition functions in Figure 6 are equal. (Note that the R -vertex of the left-hand side is ζ_k while the one on the right-hand side is ζ_{k+1} .) Then the auxiliary Yang-Baxter equations in (16) induce a solution to the Yang-Baxter equation in (14) for the fused system.*

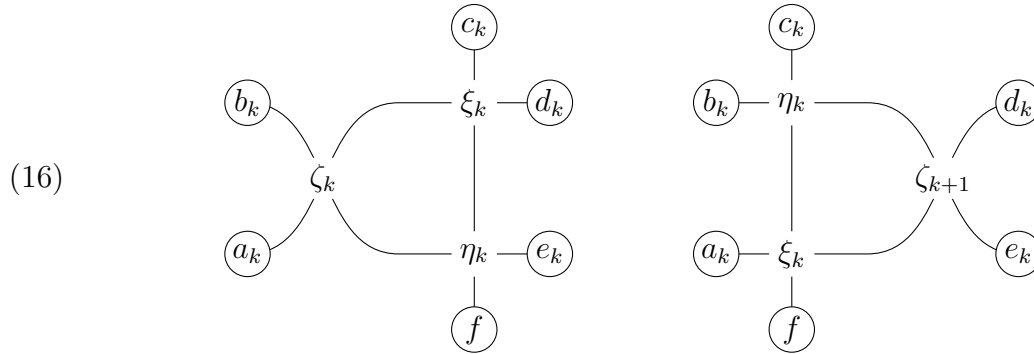


FIGURE 6. Auxiliary Yang-Baxter equations. These imply a Yang-Baxter equation for the fusion situation in Figure 5. In these equations, the R -matrix changes after moving past the vertical edges. After m such changes, it is back to its original form.

Proof. This follows from the usual train argument. Each time the R-matrix moves to the right, ζ_k is replaced by ζ_{k+1} . Since $\zeta_1 = \zeta_{m+1} = \zeta$, the statement follows. \square

Remark 3.5. We have chosen to call the method for producing new solutions to the Yang-Baxter equation outlined in this section ‘fusion,’ despite some differences with the prior notion in the literature (see for example [28] and Appendix B of [3]). Both methods construct new solutions from old by forming new weights using one-row partition functions. The typical fusion construction features two steps: first summing over all one-row systems with given multiset of spins on its vertical edges (which is the graphical manifestation of the R-matrix of a tensor product of quantum group modules) and then taking a further weighted average (which manifests the resulting R-matrix for projection onto irreducible constituents of the tensor product; see for example (B.2.1) of [3]). However, our fusion prescribes a set of labels for each vertex in the one-row system, our weights are allowed to vary based on the label, and we do not require a second summation acting as a projection. Our example of weights for fusion in the next section (see Figure 10) will have vertices labeled by colors and the weights depend critically on this color.

4. SOME YANG-BAXTER EQUATIONS

The spherical Whittaker function for $GL_r(F)$ can be expressed as the partition function of what will be called the Tokuyama model or the *uncolored* model. In the uncolored model, all edges have spins from the two element set $\Sigma := \{\oplus, \ominus\}$. As in the prior section, there are two types of vertices called ‘ordinary’ and ‘R-vertices.’ The ordinary vertices are labeled by a single complex parameter z_i , and it adjoins two horizontal and two vertical edges. We define its Boltzmann weights as in Figure 7 and let $T_{z_i} = T(z_i)$ be the associated endomorphism of $V \otimes V$, where V is the two-dimensional vector space with basis indexed by $\{\oplus, \ominus\}$. The R-vertices are labeled by a pair of complex parameters (z_i, z_j) and adjoin four horizontal edges. The Boltzmann weights are in Figure 8, and the associated endomorphism of $V \otimes V$ is denoted $R_{z_i, z_j} = R(z_i, z_j)$.

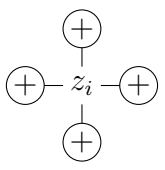
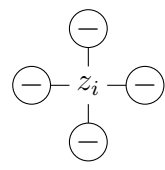
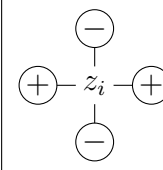
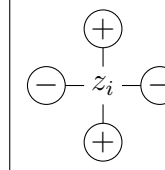
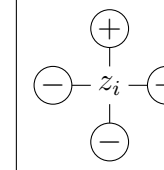
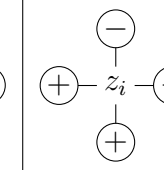
\mathbf{a}_1	\mathbf{a}_2	\mathbf{b}_1	\mathbf{b}_2	\mathbf{c}_1	\mathbf{c}_2
					
1	z_i	$-v$	z_i	$(1 - v)z_i$	1

FIGURE 7. Boltzmann weights for the Tokuyama, or uncolored, model. If a configuration of spins does not appear in this table, the Boltzmann weight is zero. The names \mathbf{a}_1 , etc. will provide a convenient shorthand for referring to admissible configurations.

Theorem 4.1. *For any choice of complex parameters (z_i, z_j) , the Boltzmann weights in Figures 7 and 8 satisfy the Yang-Baxter equation. More precisely, as endomorphisms of $V \otimes V \otimes V$,*

$$(17) \quad R(z_i, z_j)_{12} T(z_i)_{13} T(z_j)_{23} = T(z_j)_{23} T(z_i)_{13} R(z_i, z_j)_{12}.$$

$z_j - vz_i$	$z_i - vz_j$	$v(z_i - z_j)$	$z_i - z_j$	$(1 - v)z_i$	$(1 - v)z_j$

FIGURE 8. R-vertices for the Tokuyama, or uncolored, model. If a configuration of spins does not appear in this table, the Boltzmann weight is zero. The associated R-matrix agrees with R-matrix of the evaluation modules $V(z_j) \otimes V(z_i)$ for the quantum superalgebra $U_{\sqrt{v}}(\widehat{\mathfrak{gl}}(1|1))$.

Proof. This is proved in [10]. □

Equation (17) is the Yang-Baxter equation shown in Figure 4 with $\xi = z_i$, $\eta = z_j$ and $\zeta = (z_i, z_j)$. Note that this is in the opposite order of [5] where $\eta = z_i$ and $\xi = z_j$.

Next we describe Yang-Baxter equations associated to systems whose edges are decorated with both spins $\{\oplus, \ominus\}$ and colors. The resulting colored systems may be roughly understood as refinements of the uncolored system above; each uncolored state will correspond to one or more colored states whose Boltzmann weights sum to the weight of the associated uncolored state.

More precisely we begin with a set, or ‘palette’ \mathfrak{P} , of r ordered colors, which may be identified with the set of integers $1 \leq c \leq r$. Edges with a \oplus spin receive no color, while edges with a \ominus spin receive one or more colors according to the following rules. For the horizontal edges, the \ominus edge gets exactly one color, so the horizontal edges have $r + 1$ possible states, \oplus or c with $c \in \mathfrak{P}$. The vertical edges can carry more than one color (in contrast to the five-vertex model we studied in [8]). Thus each vertical edge is decorated by a subset of \mathfrak{P} , where the empty set \emptyset corresponds to the spin \oplus , so there are 2^r possible decorations.

Having described the admissible configurations at each vertex, it remains to describe the Boltzmann weights for both the ordinary and the R-vertices in colored systems. The Boltzmann weights of the R-vertex are given in Figure 9. Written in an R-matrix, these may be identified with the (ungraded) R-matrix of evaluation modules $V(z_j) \otimes V(z_i)$ for the quantum affine Lie superalgebra $U_{\sqrt{v}}(\widehat{\mathfrak{gl}}(r|1))$ (cf. [26, Definition 2.1]). The r colored \ominus spins span one graded piece in the super vector space, while the \oplus spin spans the remaining one-dimensional piece.

The Boltzmann weights of the ordinary vertices, which adjoin two horizontal edges and two vertical edges with many coloring possibilities, are harder to describe. We will define these by means of fusion, starting with simpler *monochrome vertices*: vertices that adjoin only *monochrome edges* that are only allowed to carry at most one particular color. Note that horizontal edges are always assumed to be monochrome, even for the original non-monochrome, or fused, vertices. Boltzmann weights for the monochrome (ordinary) vertices are given in Figure 10.

Convention 4.2 (Monochrome vertices). Now the admissible ordinary vertices and their weights may be described by fusion of monochrome vertices. In a model with r colors, we

replace each ordinary vertex by a single row of r monochrome vertices with color labels arranged in ascending order from left to right.

Remark 4.3. Looking ahead to Section 5, we will consider systems made from the fused vertices. Regarding the vertex as a fusion, we may replace the entire system by an *expanded* or monochrome system with monochrome vertices; each vertex is replaced by r different vertices. Then we may refer to the system with fused edges as the *fused* system. Recall that a vertical edge E adjacent to the fused vertex is decorated by a subset S_E of \mathfrak{P} . So in the expanded system, we color the c -th such edge (with color c) if and only if the color c appears in the set S_E . See Figure 19 for an example of this procedure. It follows from the definition of the fused weights that the fused and expanded systems have the same partition

$z_j - vz_i$	$z_i - vz_j$	$(1-v)z_i$ if $c < d$ $(1-v)z_j$ if $c > d$	$z_i - z_j$ if $c > d$ $v(z_i - z_j)$ if $c < d$
$(1-v)z_i$	$(1-v)z_j$	$v(z_i - z_j)$	$z_i - z_j$

FIGURE 9. The colored R-vertex weights. The colors c and d in $[1, r]$ are an arbitrary choice of distinct colors in \mathfrak{P} . If a configuration does not appear in this table, the Boltzmann weight is zero. The associated R-matrix equals that of evaluation modules $V(z_j) \otimes V(z_i)$ of the quantum supergroup $U_{\sqrt{v}}(\widehat{\mathfrak{gl}}(r|1))$.

1	z_i if $d = c$ v if $c > d$ 1 if $c < d$	$-v$	z_i if $c = d$ 1 otherwise	$(1-v)z_i$	1

FIGURE 10. Boltzmann weights for monochrome ordinary vertices. The weight depends on a pair of labels: a complex number z_i (suppressed in pictures above) and a color (denoted c above). Note that admissible vertical edges adjacent to the monochrome vertex may only carry the color c of the vertex, while adjacent horizontal edges may carry any color. In particular, in the diagrams above, $c = d$ is allowed.

function. Indeed, there is a bijection between the states of the fused and expanded systems, and corresponding states have the same Boltzmann weight, by definition.

As mentioned above, the Boltzmann weight of the fused vertex is just the partition function of the single row of these ordered r monochrome vertices, which has at most one admissible state. In Figure 11, we compute an example of a fused Boltzmann weight when $r = 2$ from the corresponding monochrome vertices. In Figure 12 we give all the fused Boltzmann weights (for any r) in which the vertical edges carry at most one color. The possible cases in which vertical edges carry two colors are shown in Figure 13. For $r > 2$ one would have to complete these with similar tables for vertical edges carrying more colors. At the end of this section we will give all the fused weights in a closed form in a notation similar to the one used in [3]. See Figure 15.

It remains to discuss the Yang-Baxter equation for fused vertices, which will result from auxiliary Yang-Baxter equations for monochrome ice according to Lemma 3.4. We first need to define monochrome R-vertices for use in (16), generalizing the R-vertices in Figure 9. These will play a role of the vertices labeled ζ_k in Lemma 3.4, but now each such R-matrix depends not only on a pair of complex parameters z_i, z_j , but also on a color c . The Boltzmann weights for these are given in Figure 14.

Let $R(z_i, z_j)$ denote the R-matrix constructed with the weights in Figure 9 according to (13), and if $1 \leq c \leq r$ is a color, let $R^{(c)}(z_i, z_j)$ denote the colored R-matrix constructed from the Boltzmann weights in Figure 14 where the vertex is labeled by the color c . Note that $R^{(1)} = R$. Also, let $T^{(c)}(z_i)$ denote the matrix associated with the monochrome (ordinary) vertices labeled by the color c whose Boltzmann weights are described in Figure 10. We recall that the colors c are identified with the integers $1 \leq c \leq r$, so there is a next color $c + 1$ unless c is the last color $c = r$, in which case we define $R^{(r+1)} := R$ to avoid writing separate cases below. We may now describe auxiliary Yang-Baxter equations involving the monochrome vertices.

Proposition 4.4. *If $1 \leq c \leq r$, then*

$$R^{(c)}(z_i, z_j)_{12} T^{(c)}(z_i)_{13} T^{(c)}(z_j)_{23} = T^{(c)}(z_j)_{23} T^{(c)}(z_i)_{13} R^{(c+1)}(z_i, z_j)_{12}.$$

Proof. Note that since we are using monochrome edges, at most three different colors can appear in the equivalent equation (16), and there are only a finite number of cases to check. This is best done using a computer. \square

Theorem 4.5. *The Yang-Baxter equation for colored models is satisfied:*

$$R(z_i, z_j)_{12} T(z_i)_{13} T(z_j)_{23} = T(z_j)_{23} T(z_i)_{13} R(z_i, z_j)_{12}$$

Proof. This follows from Proposition 4.4 and Lemma 3.4. \square

We will now describe the fused weights in a closed form. For comparison with [3], we will choose a notation close to theirs. In [3], vertical edges are labeled by tuples $\mathbf{I} = (I_1, \dots, I_r) \in \mathbb{N}^r$ representing a state in which the k -th color has multiplicity I_k . The principal difference between their systems and ours is that colors can only occur with multiplicity 0 or 1 in our systems. In other words, if we imitate their setup, each $I_k \in \{0, 1\}$. Hence the same data can be specified by the subset $\Sigma = \{k \mid I_k = 1\}$ of the palette \mathfrak{P} .

In [3], an operation adds (resp. removes) a color a to the tuple \mathbf{I} , that is, increments (resp. decrements) I_a and the resulting tuple is denoted \mathbf{I}_a^+ (resp. \mathbf{I}_a^-). We therefore introduce

$(1-v)z_i$ if $c > d$, $(-v)(1-v)z_i$ if $c < d$.	left: 1 right: $(1-v)z_i$	left: $(1-v)z_i$ right: $-v$

FIGURE 11. Colored vertex constructed from monochrome vertices by fusion for $r = 2$. Left: a fused vertex (compare with Figure 13). Middle: The case $c > d$, using weights from Figure 10. Right: The case $d > c$.

1	z_i	z_i if $c > d$ vz_i if $c < d$	$(1-v)z_i$ if $c > d$ 0 if $c < d$
$-v$	z_i	1	$(1-v)z_i$

FIGURE 12. Colored weights (I). These are the Boltzmann weights in which the vertical edges carry no more than one color. Since edges can carry more than one color, this is not a complete list of the possibilities. In this figure, $c \neq d$ except where explicitly allowed.

$(1-v)z_i$ if $c > d$, $(-v)(1-v)z_i$ if $c < d$.	v if $c > d$, $-v$ if $c < d$.	$(-v)^2$	z_i if $c > d$, vz_i if $c < d$.

FIGURE 13. Colored weights (II). The vertical edges can carry more than one color, with multiplicity at most one (so $c \neq d$ in this figure). These are the extra possibilities when at most two colors appear.

$z_j - vz_i$	$z_i - vz_j$ $c = d$ allowed.	$v(z_i - z_j)$ if $e > d$ $z_i - z_j$ if $d > e$ $c = d$ or e allowed	$(1 - v)z_j$ if $e > c > d$ or $c > d > e$ or $d > e > c$ $(1 - v)z_i$ if $d > c > e$ or $c > e > d$ or $e > d > c$
$(1 - v)z_j$	$(1 - v)z_i$	$v(z_i - z_j)$ $c = d$ allowed	$z_i - z_j$ $c = d$ allowed
	$(1 - v)z_i$ $c = d$ allowed	$(1 - v)z_j$ $c = d$ allowed	

FIGURE 14. R-vertices for auxiliary Yang-Baxter equations. These are labeled by a color c and a pair of parameters (z_i, z_j) (suppressed in the pictures above). If the color c is minimal, that is if $c \leq d, e$ for all colors that appear in this figure, this agrees with the R-vertices in Figure 9. In this figure, the colors c, d, e are distinct except when $c = d$ or $c = e$ is explicitly allowed.

the corresponding operations on the set Σ and denote $\Sigma_a^+ = \Sigma \cup \{a\}$, to be used only if $a \notin \Sigma$, and $\Sigma_a^- = \Sigma \setminus \{a\}$, to be used only if $a \in \Sigma$. Finally if $a \in \Sigma$ and $b \notin \Sigma$, we will denote $\Sigma_{ab}^{+-} = \Sigma \cup \{a\} \setminus \{b\}$, also corresponding to the \mathbf{I}_{ab}^{+-} in [3]. If $1 \leq a \leq b \leq r$, we will define $\Sigma_{[a,b]} = \{c \in \Sigma \mid a \leq c \leq b\}$.

In Figure 15 we give our Boltzmann weights in closed form using these notations. It is easy to see that these are the correct weights obtained from the monochrome weights by fusion.

Remark 4.6. The weights in Figure 15 closely resemble weights presented in Section 2.2 of [3]. One important distinction is that our weights are ‘fermionic’ — we do not allow multiple copies of any given color on an edge — while their weights are ‘bosonic’ (allowing multiplicities). Nevertheless, we may compare the weights of the multiplicity-free colored vertices in [3] with those in Figure 15; even allowing for changes of variables and Drinfeld twisting, small differences persist. For example, we may take the mirror image of the weights in [3] (2.2.2) specialized by setting $s = 0$ and compare to the weights in Figure 15 by making

$\begin{array}{c} \Sigma \\ \\ + \text{---} \text{---} + \\ \\ \Sigma \end{array}$ $(-v)^{ \Sigma_{[1,r]} }$	$\begin{array}{c} \Sigma \\ \\ c \text{---} \text{---} c \\ \\ \Sigma \end{array}$ $z_i v^{ \Sigma_{[c+1,r]} }$	$\begin{array}{c} \Sigma \\ \\ + \text{---} \text{---} c \\ \\ \Sigma_c^- \end{array}$ $(-v)^{ \Sigma_{[1,c-1]} } v^{ \Sigma_{[c+1,r]} }$
$\begin{array}{c} \Sigma \\ \\ c \text{---} \text{---} + \\ \\ \Sigma_c^+ \end{array}$ $(1-v) z_i (-v)^{ \Sigma_{[c+1,r]} }$	$\begin{array}{c} \Sigma \\ \\ c \text{---} \text{---} d \\ \\ \Sigma_{cd}^{+-} \end{array}$ $(1-v) z_i (-v)^{ \Sigma_{[c+1,d-1]} } v^{ \Sigma_{[d+1,r]} }$	$\begin{array}{c} \Sigma \\ \\ d \text{---} \text{---} c \\ \\ \Sigma_{dc}^{+-} \end{array}$ 0

FIGURE 15. Colored Boltzmann weights in a style resembling [3] (2.2.2) or (2.2.6), except that we are using + for the ‘colorless’ horizontal edges, and in place of their multiset \mathbf{I} of colors, we use a subset Σ of the palette. We are assuming $c < d$.

the substitutions $v = q^{-1}$ and $z_i = x$. Note that if no color occurs more than once on the top boundary then no vertical edge on the interior of the grid will ever have a color with multiplicity larger than one, so that the distinction between bosonic and fermionic weights becomes unimportant. Then both weight schemes have the same admissible vertices grouped into types as in Figure 15. Upon Drinfeld twisting, the Boltzmann weights agree in their powers of x and $(1 - q^{-1})$ but differ by various factors of -1 and q that cannot be resolved. Furthermore, although we have noted that bosonic weights can be excluded by imposing boundary conditions they are still important for the Yang-Baxter equation, so the R-matrices for [3] and for our system must definitely be different. We will return to the comparison of our models with [3] in Section 7.

5. COLORED SYSTEMS, FUNCTIONAL EQUATIONS AND WHITTAKER FUNCTIONS

We now describe a family of statistical-mechanical systems made from fused vertices whose partition functions may be shown to give values of Iwahori Whittaker functions in the case $G = \text{GL}_r$. Indeed, if $g \in \text{GL}_r(F)$, where F is a nonarchimedean local field, we will see the Whittaker function $\phi_w(g)$ defined by (2) can be represented as the partition function of such a model. First note that using the transformation properties of ϕ_w with respect to $N(F)$ on the left and J on the right, we may assume that g is of the form $\varpi^{-\lambda} w_2$ for some weight λ and Weyl group element w_2 . By Lemma 2.1, we may assume that λ is w_2 -almost dominant.

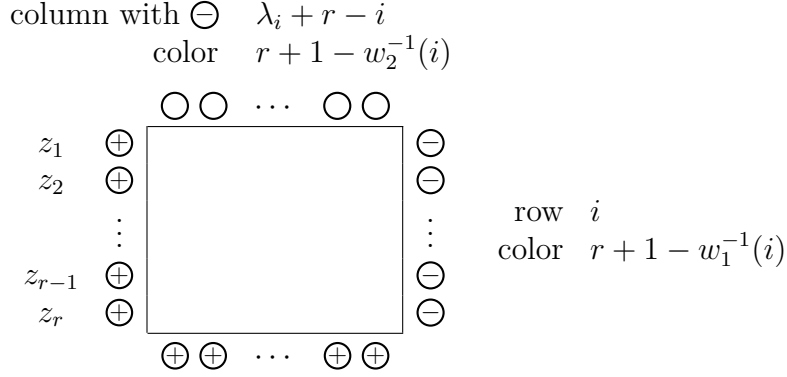


FIGURE 16. Summary of boundary conditions for $\mathfrak{S}_{\mathbf{z}, \lambda, w_1, w_2}$. On the top boundary the minus signs are positioned at columns $\lambda_i + r - i$ with color $r + 1 - w_2^{-1}(i)$ including multiplicities of colors. For the right boundary, row i is colored by $r + 1 - w_1^{-1}(i)$, each \ominus spin with only a single color.

Finally, multiplying g by an element of the center simply multiplies $\phi_w(g)$ by a scalar, so we may assume with no loss of generality that the entries in λ are nonnegative.

Having already explained how the Boltzmann weights for fused vertices are defined, it remains to explain the boundary conditions for the model and the labels on each of the vertices. For any positive integer r , the boundary conditions and vertex labels depend on three pieces of data: a partition denoted $\lambda + \rho$ with at most r nonzero parts, a pair of permutations $w_1, w_2 \in S_r = W$, the Weyl group of GL_r , and a set of r complex parameters $\mathbf{z} = (z_1, \dots, z_r)$. The systems we present here, denoted $\mathfrak{S}_{\mathbf{z}, \lambda, w_1, w_2}$ and referred to as ‘colored ice,’ may be considered as simultaneous generalizations of those appearing previously in [10] and in the colored systems of [8]. Our goal in this section is to equate the partition function of $\mathfrak{S}_{\mathbf{z}, \lambda, w_1, w_2}$ with the value of the Whittaker function $\phi_{w_1}(\mathbf{z}; \varpi^{-\lambda} w_2)$ of Section 2.

With r fixed, let $\rho = (r - 1, \dots, 1, 0)$ and let $\lambda + \rho = (\lambda_1 + r - 1, \dots, \lambda_r)$ be a partition, whose parts are written in weakly decreasing order as usual. In the identification of the weight lattice of GL_r with \mathbb{Z}^r , the corresponding weight λ satisfies $\langle \alpha, \lambda \rangle \geq -1$ for all simple roots α , a necessary condition for the non-vanishing of the Whittaker function according to Lemma 2.1.

Given the partition $\lambda + \rho$, we form a rectangular lattice consisting of $N + 1$ columns and r rows, where N is any integer at least $\lambda_1 + r - 1$. The columns will be numbered from left to right from N to 0 in decreasing order. The rows are numbered 1 to r , in increasing order from top to bottom. Given \mathbf{z} , each vertex in the i -th row receives the label z_i . The Boltzmann weights are the fused weights in Figure 15. Unless otherwise stated we will henceforth assume that the parameter v appearing in the Boltzmann weights (as well as in the Demazure-Whittaker operators among other places) equals q^{-1} with q the cardinality of the residue field of F . We will prefer the use of v to avoid confusion in later sections where, to follow tradition, q will have another meaning.

It remains to describe the boundary spins and colors located around the edge of the rectangular grid. They depend on the choice of the weight λ and the two Weyl group elements w_1, w_2 as follows and summarized in Figure 16. We have colors numbered $1, \dots, r$ at our disposal. For the top boundary, we put a \ominus spin and color $r + 1 - w_2^{-1}(i)$ on the edge in

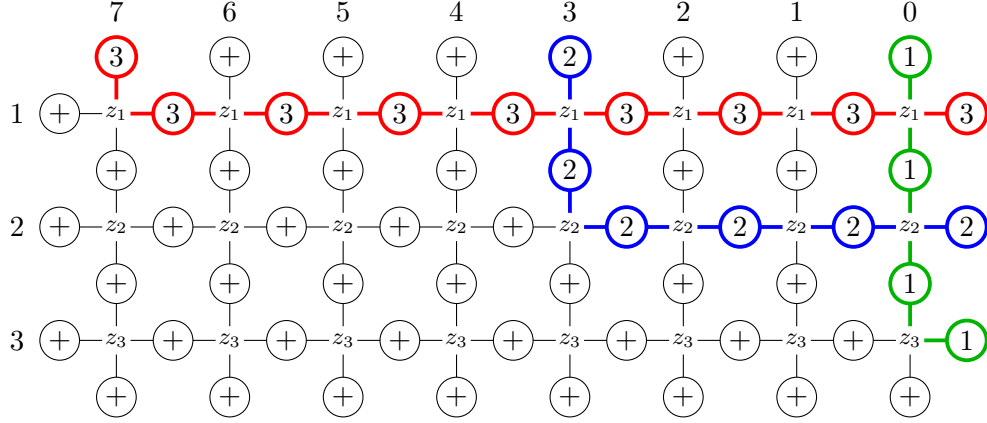


FIGURE 17. The ground state. Here $r = 3$, $\lambda = (5, 2, 0)$ so $\lambda + \rho = (7, 3, 0)$, $w_1 = w_2 = 1$ (the identity permutation), and $\mathbf{z} = (z_1, z_2, z_3)$ is an arbitrary triple of complex numbers. The top row colors read from left to right are (3, 2, 1). The colors on the right edge, read from top to bottom, are also (3, 2, 1). This is the unique state of the system $\mathfrak{S}_{\mathbf{z}, \lambda, 1, 1}$. Its Boltzmann weight is $\mathbf{z}^{\lambda + \rho}$.

the column labeled $\lambda_i + r - i$ for each $i \in \{1, \dots, r\}$ and a \oplus spin in the remaining columns. That is, we color each edge whose column index is a part of $\lambda + \rho$ and we have multiple colors on a given top boundary edge according to the multiplicity of parts in the partition. Then, we put a \oplus spin on all the left and bottom boundary edges. This leaves the right boundary edges to be described. These will depend on the choice of permutation $w_1 \in W$ for the system. All right boundary edges get a \ominus spin; moreover, the right boundary edge in the i -th row gets the color $r + 1 - w_1^{-1}(i)$. For $w_2 = 1$, these boundary conditions are exactly as in [8]. A particularly simple admissible state in a system of ‘colored ice’ is given in Figure 17.

In any state of the system $\mathfrak{S}_{\mathbf{z}, \lambda, w_1, w_2}$, the edges of any one particular color form a line (or ‘path’) starting at the top boundary and ending at the right boundary. This depiction of admissible states as configurations of lines is present in many works on lattice models, for example Baxter’s book [1], Chapter 8. The idea of using *colored* lines and refined systems that specify starting and ending points of each colored line is presented in [3]. We exploited this idea in a prior paper [8] to give a new theory of Demazure atoms, nonsymmetric pieces of Schur functions. The colored weights in this paper specialize to those of [8] by setting $v = 0$, which leads to a vast simplification. In particular every edge in [8] may carry at most one color (even in the fused model) and two colored lines can cross at most once. In this paper, weights and subsequent Yang-Baxter equations are understood via fusion, and two colored lines can cross more than once.

Let $Z_{w_1}(\mathbf{z}; \lambda, w_2)$ denote the partition function of the system $\mathfrak{S}_{\mathbf{z}, \lambda, w_1, w_2}$. We will now demonstrate that this partition function satisfies the same functional equation as the Iwahori Whittaker function ϕ_{w_1} in Proposition 2.4 under Demazure-Whittaker operators using the Yang-Baxter equation. It will be convenient to conjugate the Demazure-Whittaker operators \mathfrak{T}_i of (8) as follows

$$(18) \quad T_i = \mathbf{z}^\rho \mathfrak{T}_i \mathbf{z}^{-\rho}.$$

such that

$$(19) \quad T_i \cdot f(\mathbf{z}) = \frac{\mathbf{z}^{\alpha_i} - v}{1 - \mathbf{z}^{\alpha_i}} f(s_i \mathbf{z}) + \frac{v - 1}{1 - \mathbf{z}^{\alpha_i}} f(\mathbf{z})$$

and

$$(20) \quad T_i^{-1} \cdot f(\mathbf{z}) = \frac{\mathbf{z}^{\alpha_i} - v}{v(1 - \mathbf{z}^{\alpha_i})} f(s_i \mathbf{z}) + \frac{(v - 1)\mathbf{z}^{\alpha_i}}{v(1 - \mathbf{z}^{\alpha_i})} f(\mathbf{z}).$$

Proposition 5.1. *For any partition $\lambda + \rho$, simple reflection s_i , and any pair of Weyl group elements $w_1, w_2 \in W$,*

$$(21) \quad Z_{s_i w_1}(\mathbf{z}; \lambda, w_2) = \begin{cases} T_i Z_{w_1}(\mathbf{z}; \lambda, w_2) & \text{if } \ell(s_i w_1) > \ell(w_1), \\ T_i^{-1} Z_{w_1}(\mathbf{z}; \lambda, w_2) & \text{if } \ell(s_i w_1) < \ell(w_1). \end{cases}$$

Proof. Repeated use of the Yang-Baxter equation gives the equality of the partition functions in Figure 18.

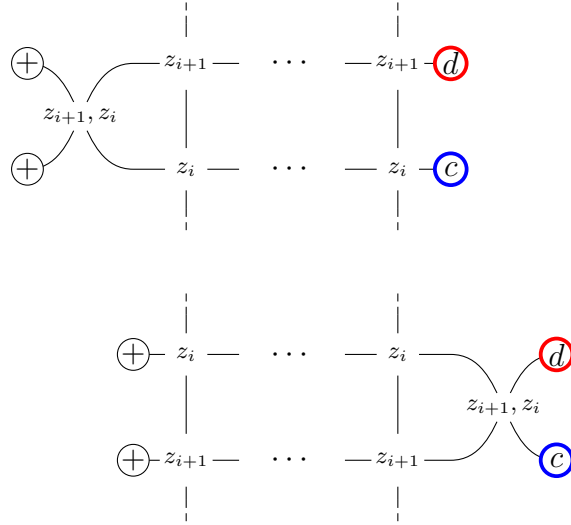


FIGURE 18. Top: the system $\mathfrak{S}_{s_i \mathbf{z}, \lambda, w_1, w_2}$ with the R-matrix attached. Bottom: after using the Yang-Baxter equation.

Using the R -matrix weights from Figure 9, we obtain the following identity of partition functions:

$$(22) \quad (z_i - v z_{i+1}) Z_{w_1}(s_i \mathbf{z}; \lambda, w_2) = \begin{cases} (1 - v) z_{i+1} Z_{w_1}(\mathbf{z}; \lambda, w_2) + (z_{i+1} - z_i) Z_{s_i w_1}(\mathbf{z}; \lambda, w_2) & \text{if } \ell(s_i w_1) > \ell(w_1), \\ (1 - v) z_i Z_{w_1}(\mathbf{z}; \lambda, w_2) + v(z_{i+1} - z_i) Z_{s_i w_1}(\mathbf{z}; \lambda, w_2) & \text{if } \ell(s_i w_1) < \ell(w_1). \end{cases}$$

Note that $s_i w > w$ is equivalent to $c > d$ in the notation of Figure 9. Consulting the table, there is one possible choice for the R-matrix for the top state in Figure 18, and two possible choices for the bottom state, accounting for the three terms in the identity (22). Note that we take (i, j) in Figure 9 to be $(i + 1, i)$.

Setting $\mathbf{z}^{\alpha_i} = z_i/z_{i+1}$, and rearranging terms in (22) upon division by z_{i+1} , we obtain the desired equality. \square

We have noted in Remark 4.3 that we may replace a system such as $\mathfrak{S}_{\mathbf{z},\lambda,w_1,w_2}$ made with fused Boltzmann weights by an equivalent system with r times as many vertices, using monochrome weights. The expanded monochrome system will appear in the following proof. See Figure 19 for an example.

Theorem 5.2. *Given any $w_1, w_2 \in W$, let λ be a w_2 -almost dominant weight with corresponding partition $\lambda + \rho$. Let $\mathfrak{S}_{\mathbf{z},\lambda,w_1,w_2}$ be the corresponding system of colored ice with associated partition function $Z_{w_1}(\mathbf{z}; \lambda, w_2)$. Then*

$$(23) \quad Z_{w_1}(\mathbf{z}; \lambda, w_2) = \mathbf{z}^\rho \phi_{w_1}(\mathbf{z}; \varpi^{-\lambda} w_2).$$

Proof. Comparing Proposition 5.1 and Proposition 2.4 while bearing in mind (18), both sides of (23) satisfy the same recursive formula, so if (23) is true for one value of w_1 , it is true for all w_1 . Thus we may assume that $w_1 = w_2$.

We will show that when $w_1 = w_2 = w$ the system has a unique state. We will use the monochrome model, in which each vertical edge has been broken into r distinct vertical edges, and the color c , if we identify c with an integer $1 \leq c \leq r$ can only be carried by the c -th such vertical edge. The following argument shows that the condition that λ is w_2 -dominant implies that the sequence of colors on the top boundary edges are the same as the sequence of colors on the right boundary edges. By definition of $\mathfrak{S}_{\mathbf{z},\lambda,w,w}$ the sequence of colors on the right edge are $r + 1 - w^{-1}(i)$. On the top edge, the color in the $\lambda_i + r - i$ column is also $r + 1 - w^{-1}(i)$, and the sequence of integers $\lambda_i + r - i$ is weakly decreasing. Since columns are labeled in decreasing order, we see that if the $\lambda_i + r - i$ are distinct, then the colors are in the same order on the top boundary and on the right boundary, as claimed. But we must consider what happens if several $\lambda_i + r - i$ are equal, as in Figure 19. If $\lambda_i + r - i = \lambda_{i+1} + r - (i + 1)$ then $\langle \lambda, \alpha_i^\vee \rangle = -1$ so our condition that λ is w -almost dominant implies that $w^{-1}\alpha_i$ is a negative root. Therefore $w^{-1}(i) > w^{-1}(i + 1)$ and so the colors on the right edge in rows $i, i + 1$ are $r + 1 - w^{-1}(i) < r + 1 - w^{-1}(i + 1)$. Now let us see that this agrees with the condition in the top. Indeed, when we split the vertices into monochrome vertices as in Convention 4.2, they are in increasing order.

We have shown that the colors in the top boundary edges of the monochrome model are in the same order as on the right boundary edges. From this it is easily deduced that there is only one possible state, and that every colored line crosses every other colored line (exactly once). We need to consider the Boltzmann weights that arise from these crossings. Consulting the second case in Figure 10 we see that when $c > d$, the crossing produces a factor of v , otherwise it does not. The total number of such crossings is the number of inversions of w^{-1} , that is $\ell(w)$. Also in the i -th row, using the ordinary (non-monochrome) colored model, the number of factors z_i will be the number of vertices with a colored edge to the left, which will be $z_i^{\lambda_i + r - i}$. Therefore the Boltzmann weight of the state is therefore $v^{\ell(w)} \mathbf{z}^{\lambda + \rho}$. By Proposition 2.2 this equals $\mathbf{z}^\rho \phi_w(\mathbf{z}, \varpi^{-\lambda} w)$, and we are done. \square

Proposition 5.3. *Let $\mu' = (\mu'_1, \dots, \mu'_r) \in \mathbb{Z}^r$. There exists a unique pair (w, λ) , with $w \in W$ and $\lambda = (\lambda_1, \dots, \lambda_r)$ a w -almost dominant weight, such that*

$$w(\mu') = \lambda + \rho.$$

Proof. We may find w and λ such that $w(\mu') = \lambda + \rho$ and $\lambda + \rho$ is dominant. Clearly λ is unique but w may not be if we only require $w(\mu')$ to be dominant. However the stronger condition that $w(\mu') - \rho$ is w -almost dominant will force w to be unique as follows.

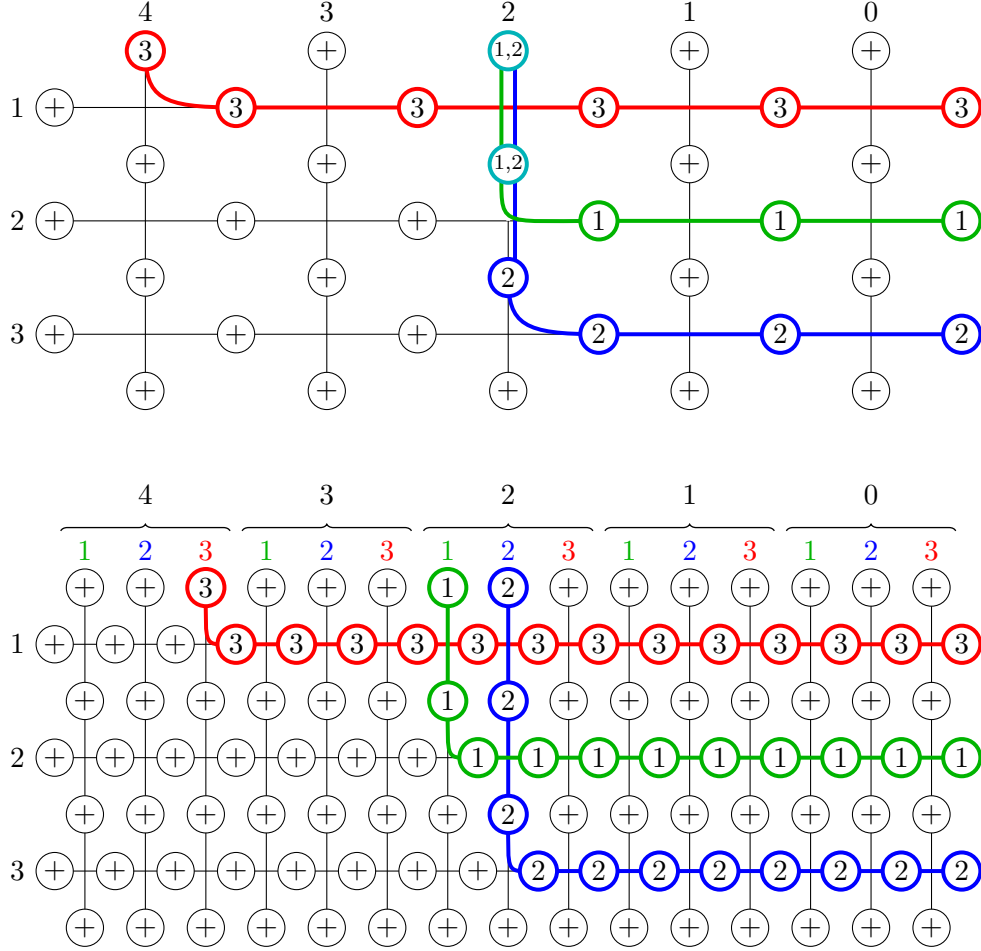


FIGURE 19. The unique state of $\mathfrak{S}_{\mathbf{z}, \lambda, w_1, w_2}$ for $G = \mathrm{GL}_3$ with $w_1 = w_2 = s_2$ in $W = S_3$ and $\lambda = (2, 1, 2)$ shown with fused vertices (top) and monochrome vertices (bottom). Note that while λ is not dominant, it is w_2 -almost dominant. The partition function $z_1^4 z_2^2 z_3^2$ of this system equals $\mathbf{z}^\rho \phi_{s_2}(\varpi^{-\lambda} s_2)$.

We recall that $w^{-1}\alpha_i \in \Delta^+$ if and only if $\ell(s_i w) > \ell(w)$. The w such that $w(\mu') = \lambda + \rho$ lie in a single left coset of the stabilizer of $\lambda + \rho$, which is a Coxeter group generated by the s_i such that $\lambda_i + 1 = \lambda_{i+1}$. But the condition that $w(\mu') - \rho$ is w -almost dominant is equivalent to the assumption that $\ell(s_i w) < \ell(w)$ whenever $\lambda_i + 1 = \lambda_{i+1}$. So this condition means that any s_i among the generators of this stabilizer is a left descent of w . Thus clearly there is a unique w in this coset such that λ is w -almost dominant, and that is the longest element of W such that $w(\mu') = \lambda + \rho$. \square

Remark 5.4. As noted above, the ‘standard basis’ of Iwahori Whittaker functions ϕ_{w_1} are determined by their values at $\varpi^{-\lambda} w_2$. We have shown in Theorem 5.2 that these values are partition functions of certain systems $\mathfrak{S}_{\mathbf{z}, \lambda, w_1, w_2}$. Proposition 5.3 shows that the partition function of every ‘colored ice’ system is a value of an Iwahori Whittaker function. Indeed, the data describing the system are colorings of the top and right boundary edges. In other words, the data are two maps from the set of colors to the top boundary edges (labeled by columns) and to the right boundary edges (labeled by rows). The map to rows is bijective

but the map to columns can be any map; as in Figure 19 it does not need to be injective. Let μ'_i be the column corresponding to the $(r+1-i)$ -th color. Applying Proposition 5.3 to $\mu' = (\mu'_1, \dots, \mu'_r)$ produces a pair (w_2, λ) such that λ is w_2 -almost dominant and $w_2\mu' = \lambda + \rho$. In column $\lambda_i + \rho_i = (w_2\mu')_i = \mu'_{w_2^{-1}(i)}$ we then have the color $r+1-w_2^{-1}(i)$ exactly as specified for the top boundary edges in Figure 16. Thus, from every μ' we obtain a system $\mathfrak{S}_{\mathbf{z}, \lambda, w_1, w_2}$ with w_1 determined by the permutation of colors on the right edge. For future reference define

$$(24) \quad \mu = w_0\mu' = w_0w_2^{-1}(\lambda + \rho),$$

which has the advantage that column μ_i has color i .

6. RELATION WITH UNCOLORED MODELS

Given a partition λ we may construct the uncolored model $\mathfrak{S}_{\mathbf{z}, \lambda}$ using the Boltzmann weights in Figure 7. The boundary conditions are the same as for the systems $\mathfrak{S}_{\mathbf{z}, \lambda, w_1, w_2}$ except that every colored boundary spin is replaced by \ominus ; in particular, the partition $\lambda + \rho$ is strictly dominant so \ominus spins along the top boundary are assigned to distinct columns. Let $Z(\mathbf{z}; \lambda)$ denote the partition function of the uncolored system. The following statement is known as ‘‘Tokuyama’s Theorem’’ since it is equivalent to the main result in [42].

Proposition 6.1. *We have*

$$Z(\mathbf{z}; \lambda) = \mathbf{z}^\rho \prod_{\alpha \in \Delta^+} (1 - v\mathbf{z}^{-\alpha}) s_\lambda(\mathbf{z}).$$

Proof. This is proved in [10] using the Yang-Baxter equation. \square

We will associate with a state of the uncolored system a Gelfand-Tsetlin pattern with top row $\lambda + \rho$. It is easy to see that in any given state \mathfrak{s} of the system, the number of \ominus spins in the row of vertical edges above the i -th row will be exactly $r+1-i$. Let j enumerate these spins and let $A_{i,j}$ be their column positions, in descending order. Then

$$\text{GTP}(\mathfrak{s}) = \left\{ \begin{array}{cccccc} A_{1,1} & & A_{1,2} & & \cdots & & A_{1,r} \\ & A_{2,2} & & \cdots & & A_{2,r} & \\ & & \ddots & \vdots & \ddots & & \\ & & & A_{r,r} & & & \end{array} \right\}$$

is a *strict Gelfand-Tsetlin pattern*, meaning that $A_{i,j} \geq A_{i+1,j+1} \geq A_{i,j+1}$ and $A_{i,j} > A_{i,j+1}$.

Lemma 6.2. *The map $\mathfrak{s} \mapsto \text{GTP}(\mathfrak{s})$ is a bijection between the states of $\mathfrak{S}_{\mathbf{z}, \lambda}$ and the strict Gelfand-Tsetlin patterns with top row $\lambda + \rho$.*

Proof. This is straightforward and also explained in [11], Chapter 19. \square

Now let us consider colored systems of the form $\mathfrak{S}_{\mathbf{z}, \lambda, w, 1}$. Let

$$\mathfrak{S}_{\mathbf{z}, \lambda, \text{colored}} = \bigsqcup_{w \in S_r} \mathfrak{S}_{\mathbf{z}, \lambda, w, 1}$$

be the disjoint union of these systems. We call a state of the colored system *strict* if no vertical edges carry more than one color. Thus the states in Figure 20 are strict, but those in Figure 21 are not.

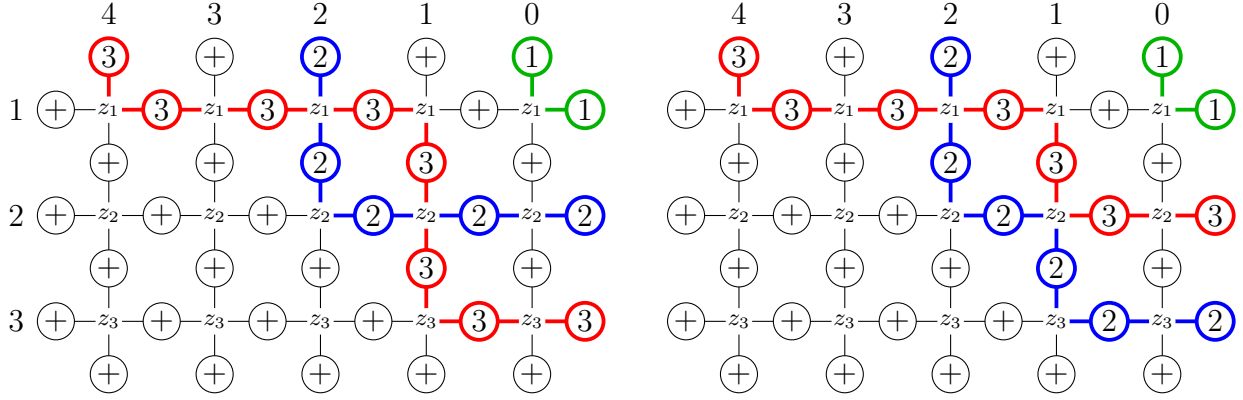


FIGURE 20. Twin states that are strict, i.e. they have no multicolored edges. These both correspond to the same uncolored state, but contribute to different Iwahori Whittaker functions.

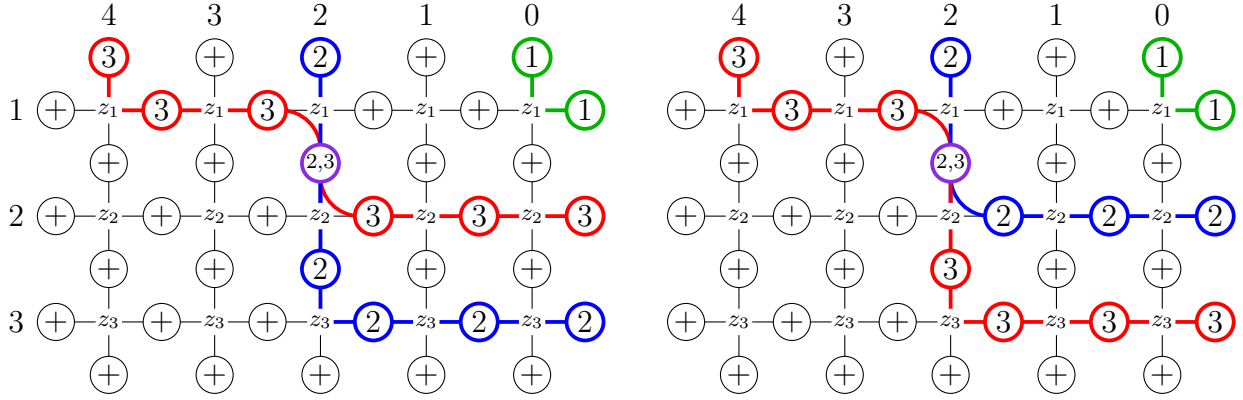


FIGURE 21. Twin states that are nonstrict (i.e. they have a multicolored edge).

We may partition the states into the disjoint union

$$\mathfrak{S}_{\mathbf{z},\lambda,\text{colored}} = \mathfrak{S}_{\mathbf{z},\lambda,\text{strict}} \sqcup \mathfrak{S}_{\mathbf{z},\lambda,\text{nonstrict}},$$

where the first set is the ensemble of strict states, and the second is the ensemble of nonstrict ones.

Now there is a map $\pi : \mathfrak{S}_{\mathbf{z},\lambda,\text{strict}} \rightarrow \mathfrak{S}_{\mathbf{z},\lambda}$ from strict colored states to uncolored ones; this map replaces every colored edge in a state with a \ominus .

Let \mathfrak{s}_0 be a state of the uncolored system, and let $\beta(\mathfrak{s}_0)$ be its Boltzmann weight obtained using Figure 7. We will show that the Boltzmann weight $\beta(\mathfrak{s}_0)$ is the sum of the Boltzmann weights of the strict states of the colored system that map to it.

Proposition 6.3. *Let \mathfrak{s}_0 be a state of the uncolored system $\mathfrak{S}_{\mathbf{z},\lambda}$. Then,*

$$\sum_{\substack{\mathfrak{s} \in \mathfrak{S}_{\mathbf{z},\lambda,\text{strict}} \\ \pi(\mathfrak{s}) = \mathfrak{s}_0}} \beta(\mathfrak{s}) = \beta(\mathfrak{s}_0).$$

Proof. Note that in a strict colored state, only configurations from Figure 12 can occur.

We begin by considering how to ‘color’ the uncolored state, meaning, to replace all the \ominus spins by colors. The top boundary \ominus edge spins must be replaced by the colors $r, r-1, \dots, 1$ in order. The top boundary \oplus spins, and the left edge boundary spins will remain \oplus .

Let us consider how to add colors to a vertex from Figure 7 with the edges labeled A, B, C, D as in Figure 2 (right). We assume that the colors of A and B are already decided (including the possibility that one of these edges is labeled \oplus so that no color is needed). We will consider the possibilities for adding colors to edges C and D consistent with Figure 12.

Except in the case of an \mathfrak{a}_2 pattern, the colors of C and D are uniquely determined, and the Boltzmann weight of the corresponding configurations from Figure 7 and Figure 12 are the same. For an \mathfrak{a}_2 pattern there is also a unique way of coloring the edges C and D with the exception of the case where (the color of edge B) $>$ (the color of edge A); in this case there are two different possible colorings for C and D , but the Boltzmann weights of the two colorings sum to z_i (where we are in the i -th row), which is the Boltzmann weight of the \mathfrak{a}_2 pattern in Figure 7.

We now see that we can enumerate the colored states \mathfrak{s} such that $\pi(\mathfrak{s}) = \mathfrak{s}_0$ as follows. Starting with the assigned colors of the top row, and the \oplus spins on the left edge, we proceed from left to right, and from top to bottom. Usually there is a unique way of assigning colors to the edges in positions C and D when the edges A and B are known; but in every case, the sum of the Boltzmann weights of possible configurations for the colored vertex equals the Boltzmann weight of the corresponding uncolored vertex. Consequently when we sum over all the possible states \mathfrak{s} that project to \mathfrak{s}_0 , we get the Boltzmann weight of the uncolored state \mathfrak{s}_0 . \square

For example, in Figure 20 we have two strict colored states that map to the same uncolored state.

Remark 6.4. It is not hard to see that, for strict states, the cases where more than one colored pattern can map to the same uncolored one are the cases where two colored lines meet more than once, as in Figure 20. The first time they meet, the lines must cross; the second time they meet, they may or may not cross as in Figure 20.

Remark 6.5. When two states \mathfrak{s} and \mathfrak{s}' map to the same uncolored state, they usually lie in colored systems $\mathfrak{S}_{\mathbf{z}, \lambda, w, 1}$ with different Weyl elements w . Hence they contribute to different Iwahori Whittaker functions ϕ_w . Again see Figure 20 for an example.

We turn now to the nonstrict states. Surprisingly, the Boltzmann weights of these states cancel. Our proof of this in Proposition 6.7 is rather indirect. It is probable that a direct proof would involve some interesting combinatorics. We will make use of the following Proposition which is a version of the Casselman-Shalika [15] formula. This is valid for any split reductive group but we only need it for GL_r .

Proposition 6.6. *For any positive integer r , let $W = S_r$ and let λ be a partition with at most r parts. Then*

$$(25) \quad \sum_{w \in W} \phi_w(\mathbf{z}; \varpi^{-\lambda}) = \prod_{\alpha \in \Delta^+} (1 - v\mathbf{z}^{-\alpha}) s_\lambda(\mathbf{z}),$$

where s_λ is the Schur polynomial.

Proof. See Theorem 2.5 of [6], or Proposition 8.2 below, which is based on [12] Theorem 14. \square

Proposition 6.7. *We have*

$$(26) \quad \sum_{\mathfrak{s} \in \mathfrak{S}_{\mathbf{z}, \lambda, \text{nonstrict}}} \beta(\mathfrak{s}) = 0.$$

Proof. By Proposition 6.3, we can sum the weights of the strict states by grouping them according to the uncolored states they project to

$$\sum_{\mathfrak{s} \in \mathfrak{S}_{\mathbf{z}, \lambda, \text{strict}}} \beta(\mathfrak{s}) = \sum_{\mathfrak{s}_0 \in \mathfrak{S}_{\mathbf{z}, \lambda}} \beta(\mathfrak{s}_0) = Z(\mathbf{z}, \lambda).$$

Therefore

$$\sum_{\mathfrak{s} \in \mathfrak{S}_{\mathbf{z}, \lambda, \text{nonstrict}}} \beta(\mathfrak{s}) = \sum_{\mathfrak{s} \in \mathfrak{S}_{\mathbf{z}, \lambda, \text{colored}}} \beta(\mathfrak{s}) - \sum_{\mathfrak{s} \in \mathfrak{S}_{\mathbf{z}, \lambda, \text{strict}}} \beta(\mathfrak{s}) = \left(\sum_{w \in W} Z_w(\mathbf{z}, \lambda, 1) \right) - Z(\mathbf{z}, \lambda).$$

Now using Theorem 5.2 and Tokuyama's formula Proposition 6.1, this equals

$$\mathbf{z}^\rho \sum_{w \in W} \phi_w(\mathbf{z}; \varpi^{-\lambda}) - \mathbf{z}^\rho \prod_{\alpha \in \Delta^+} (1 - v\mathbf{z}^{-\alpha}) s_\lambda(\mathbf{z})$$

and by Proposition 6.6 this is zero. \square

Remark 6.8. Proposition 6.7 shows that the contribution of the nonstrict states to the *spherical* Whittaker function is zero. However for the Iwahori Whittaker functions, they cannot be ignored. See Figure 21 for an example of two nonstrict states whose Boltzmann weights cancel; but they lie in different systems $\mathfrak{S}_{\mathbf{z}, \lambda, w, 1}$, and so they contribute to different Iwahori Whittaker functions.

Although the nonstrict states do not map to states of the uncolored model, we may nevertheless extend the map GTP to map them to Gelfand-Tsetlin patterns with top row $\lambda + \rho$. The entries in the k -th row of $\text{GTP}(\mathfrak{s})$ are the numbers of the columns that carry a colored vertical edge, and the number of times a column number appears is the number of colors that that vertical edge carries. If \mathfrak{s} is any state, then $\text{GTP}(\mathfrak{s})$ is a strict Gelfand-Tsetlin pattern if and only if \mathfrak{s} is strict. We conjecture that if Γ is any fixed nonstrict Gelfand-Tsetlin pattern then the sum of the Boltzmann weights of \mathfrak{s} such that $\text{GTP}(\mathfrak{s}) = \Gamma$ is zero. This would refine Proposition 6.7.

7. RELATIONSHIP WITH BORODIN-WHEELER MODELS

In this section we will show that the Boltzmann weights for admissible states in our models can be related to a subset of weights of models described in [3]. This implies relations between the partition functions of this paper and of [3].

The models in this paper and in [3] differ in one important aspect: in this paper the vertical edges can carry more than one color, but no color can have a multiplicity greater than 1. In [3], the vertical edges can have greater multiplicity of color. The vertical edges in our paper are thus ‘fermionic’ and those in [3] are ‘bosonic’ (allowing superposition of particles). Uncolored bosonic models appear earlier in [27, 2, 43].

Moreover, the relevant R-matrices from each solvable model are different, corresponding to different quantum groups. Up to twisting, the R-matrix in [3] is associated with the quantum group for $\widehat{\mathfrak{sl}}(r+1)$, whereas in this paper, the R-matrix is associated with the quantum super group for $\widehat{\mathfrak{gl}}(r|1)$. Nevertheless, the two sets of weights are comparable if we choose boundary conditions such that states with bosonic color multiplicities can never occur. (This

is achieved simply by never using a color more than once on the top boundary edges.) Then the great surprise is that, despite the above differences in the models, the resulting states in the fermionic and bosonic models can be compared termwise leading to an identity (28) between the two partition functions. A similar phenomenon is noted in Remark 4.3 of [8].

This correspondence does not extend to the uncolored models. For when we pass to the uncolored models, the partition functions for both models become symmetric functions, but now they are different. Indeed, we will show in Section 8 that we get $\sum_w \mathfrak{F}_w \mathbf{z}^\lambda$ in the fermionic (Tokuyama) case and $\sum_w \mathfrak{L}_w \mathbf{z}^\lambda$ in the bosonic case. By Proposition 8.2 below these are, respectively, a Schur function times a deformed Weyl denominator, and a Hall-Littlewood polynomial.

We will now show a relationship between our Boltzmann weights in Figure 15 and a transformed version of the Boltzmann weights from Borodin-Wheeler in (2.2.2) of [3], but first we need the following notion.

We define a ‘crossing’ (of colors at a vertex) to be an orthogonal crossing of two colored paths at the vertex in the corresponding monochrome state of the model. So for example in Figure 19, a state and its associated monochrome state are presented and the number of crossings for the vertex in row 1 and column 2 is two, while the number of crossings at row 2 and column 2 is one. As another example, in the fourth frame of Figure 22 the number of crossings at the vertex is $|\Sigma_{[1,c-1]}|$ according to the associated monochrome model.

Proposition 7.1. *Consider the fermionic restriction of the weights of Borodin-Wheeler in [3, (2.2.2)], that is, with color multiplicities at most one. Reflect each weight in the vertical axis, reverse the color palette such that color i maps to color $r + 1 - i$ (which also reverses the ordering), and let their $q = v^{-1}$, $x_i = z_i$ and $s = 0$. Then the ratio of our Boltzmann weights in Figure 15 over these transformed weights is*

$$(27) \quad (-v)^{|\Sigma|} (-1)^{\#\text{crossings at vertex}}$$

where Σ is the set of colors in the bottom edge.

Proof. This is readily checked by comparing the weights in Figure 22 which shows our weights and the transformed weights of Borodin-Wheeler. Note that reversing the color palette has the effect that $I_{i+1,n}$ in their table will be replaced by $I_{1,i-1}$ (or $\Sigma_{1,i-1}$ in our notation). Their n is our r , the number of colors. \square

Given any weight μ , let $f_\mu(x_1, \dots, x_r; q, s) := f_\mu(x_1, \dots, x_r)$ be the partition function in [3, (3.4.4) and (3.4.5)]. We use this verbose notation to declare the parameters q and s used to describe the Boltzmann weights in (2.2.2) of [3] that define f_μ . Here w_0 is the long Weyl group element.

Theorem 7.2. *Assume that λ is dominant and $w_2 \leq w_1$. Then:*

$$(28) \quad Z_{w_1}(\mathbf{z}; \lambda, w_2) = v^{\ell(w_1)} (-1)^{\ell(w_1 w_2^{-1})} w_0 f_{w_0 w_1 w_2^{-1}(\lambda+\rho)}(z_1, \dots, z_r; v^{-1}, 0).$$

Proof. We note that Corollary 2.6 and Theorem 5.2 imply (when $w_2 \leq w_1$) the identity

$$Z_{w_0}(\mathbf{z}; \lambda, w_2 w_1^{-1} w_0) = v^{\ell(w_1^{-1} w_2)} Z_{w_1}(\mathbf{z}; \lambda, w_2).$$

Hence we are reduced to proving the special case

$$(29) \quad Z_{w_0}(\mathbf{z}; \lambda, w_2) = (-v)^{\ell(w_0)} (-1)^{\ell(w_2)} w_0 f_{w_2^{-1}(\lambda+\rho)}(\mathbf{z}; v^{-1}, 0).$$

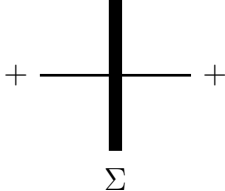
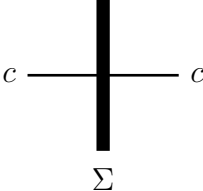
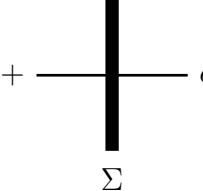
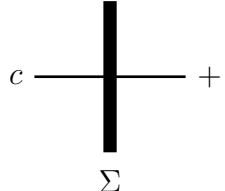
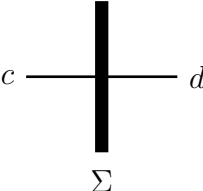
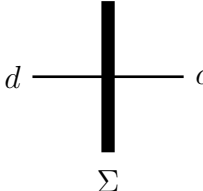
Σ  Σ	Σ  Σ	Σ_c^+  Σ
$(-v)^{ \Sigma_{[1,r]} }$	$zv^{ \Sigma_{[c+1,r]} }$	$(-v)^{ \Sigma_{[1,c-1]} }v^{ \Sigma_{[c+1,r]} }$
1	$xq^{ \Sigma_{[1,c-1]} }$	1
Σ_c^-  Σ	Σ_{dc}^{+-}  Σ	Σ_c^{+-}  Σ
$(1-v)z(-v)^{ \Sigma_{[c+1,r]} }$	$(1-v)z(-v)^{ \Sigma_{[c+1,d-1]} }v^{ \Sigma_{[d+1,r]} }$	0
$x(1-q)q^{ \Sigma_{[1,c-1]} }$	$x(1-q)q^{ \Sigma_{[1,d-1]} }$	0

FIGURE 22. Colored Boltzmann weights in this paper (middle row) and in [3] (2.2.2) slightly modified (bottom row). For the [3] we take their parameter $s = 0$, and then we make the following modifications. First, we mirror reflect the vertex left-to-right, and second, we reverse the order of the colors. Here we continue to use $+$ for the ‘colorless’ horizontal edges, and Σ is a subset of the color palette. We are assuming $c < d$. The respective spectral parameters are x and z .

We will prove (29) by relating our system $\mathfrak{S}_{\mathbf{z},\lambda,w_0,w_2}$ representing $Z_{w_0}(\mathbf{z}; \lambda, w_2)$ to the system of [3, (3.4.5)] representing f_μ using (the inverse of) the map described in Proposition 7.1. We start by discussing how the boundary conditions for $\mathfrak{S}_{\mathbf{z},\lambda,w_0,w_2}$ are mapped under this transformation. With $w_1 = w_0$, the colors on the right boundary are $(1, \dots, r)$ from top-to-bottom. Let $\mu = w_0 w_2^{-1}(\lambda + \rho)$ as in (24) describe the top boundary such that column μ_i has color i .

The columns in [3, (3.4.5)] are labeled in increasing order from left-to-right while our columns are labeled from right-to-left. Thus, with this change of conventions, the reflection in the vertical axis leaves μ unchanged while the color reversal maps μ to $w_0 \mu = w_2^{-1}(\lambda + \rho)$. The bottom boundary is unchanged and the same for the two models.

The right boundary condition of $\mathfrak{S}_{\mathbf{z},\lambda,w_0,w_2}$ is mapped to the left boundary condition of [3, (3.4.5)] with colors $(1, \dots, r)$ from bottom-to-top under the reflection and the color reversal, and the remaining boundary is trivially identified under the map. We have thus shown that the boundary conditions of $\mathfrak{S}_{\mathbf{z},\lambda,w_0,w_2}$ map to exactly the boundary conditions of $f_{w_2^{-1}(\lambda + \rho)}$ in [3, (3.4.5)].

With this dictionary between the boundary conditions of the two systems together with Proposition 7.1, we have a bijection of states between the two systems. Recall that restricting

the colors of the boundary in [3, (3.4.5)] to be at most of multiplicity one implies that all vertical edges in the state have colors of multiplicity at most one. Simultaneously changing the boundary conditions and the Boltzmann weights of the Borodin-Wheeler system under the map in Proposition 7.1 is effectively a rewriting of the original system and does not change the partition function.

Using Proposition 7.1, we will now show that the ratio between the total Boltzmann weights of corresponding states under the bijection is

$$(30) \quad (-v)^{\ell(w_0)}(-1)^{\ell(w_2)}.$$

The ratio for the states is the product of the ratios for the involved vertices which is given by (27), and the sum over all vertices of $|\Sigma|$ is $\frac{1}{2}r(r-1) = \ell(w_0)$. Since $\lambda + \rho$ is strictly dominant and $\mu = w_0 w_2^{-1}(\lambda + \rho)$ assigns the color i to column μ_i , the order of the colors on the top boundary of $\mathfrak{S}_{\mathbf{z}, \lambda, w_0, w_2}$ from left-to-right is $w_0 w_2^{-1}(1, \dots, r)$. As mentioned above, the order of colors from top-to-bottom on the right boundary is simply $(1, \dots, r)$. Thus, the total number of crossings is congruent to $\ell(w_2)$ modulo 2. (It is exactly $\ell(w_2)$ if no two lines cross more than once.) Together, we get the global ratio (30).

Equation (29) now follows by summing all states. The application of w_0 to $f_{w_2^{-1}(\lambda+\rho)}(\mathbf{z}; v^{-1}, 0)$ is required because the order of the spectral parameters is reversed. \square

Remark 7.3. It is remarkable that Proposition 7.1 gives a state-by-state comparison between the functions f_μ in [3] and certain of our $Z_{w_1}(\mathbf{z}; \lambda, w_2)$. Both are known to be specializations of non-symmetric Macdonald polynomials as we discuss in Section 8.

More general results than Theorem 7.2 are also possible, using slightly more exotic functions. Indeed in (3.5.1) of [3], they define functions $f_\mu^w(\mathbf{z}; q, s)$ that generalize the $f_\mu(\mathbf{z}; q, s)$ above. For us the relevant point is that for any i , $-T_i^{-1} f_\mu^w(\mathbf{z}) = f_\mu^{s_i w}(\mathbf{z})$ according to [3] (5.3.2) with T_i^{-1} as in (20) and $v = q^{-1}$ as usual. Thus combining (21) with (29), one may immediately conclude that for any $w_1, w_2 \in W$:

$$Z_{w_1 w_0}(\mathbf{z}; \lambda, w_2) = (-v)^{\ell(w_0)}(-1)^{\ell(w_1 w_2)} w_0 f_{w_2^{-1}(\lambda+\rho)}^{w_1}(\mathbf{z}; v^{-1}, 0).$$

8. NONSYMMETRIC MACDONALD POLYNOMIALS

Nonsymmetric Macdonald polynomials depend on two parameters which are usually denoted q and t . There are differing notations in the literature, but in this paper we will follow the notation $E_\lambda(\mathbf{z}; q, t)$ of Haglund, Haiman and Loehr [21]. Note that q is here not related to the cardinality of the residue field of F ; we will, in this section, instead solely use v^{-1} for this quantity. In fact, the t of [21] equals our v which is the parameter appearing in the quadratic Hecke relations below.

Remark 8.1. We caution the reader that there are several different notations for nonsymmetric Macdonald polynomials. The notation in [21] that we will follow differs from that used in [3, 4]. In particular, since we will compare our results with those of [3] we note that in our notation (and that of Haglund, Haiman and Loehr) their identity (5.9.15) would be written

$$f_\mu(x_1, \dots, x_n; q, s)|_{s=0} = E_\mu(x_1, \dots, x_n; \infty, 1/q).$$

The second parameter in E_μ is the one usually denoted t in the literature. Thus the relevant specialization is $(q, t) = (\infty, 1/q)$.

If $q = 0$ or ∞ the polynomials $E_\lambda(\mathbf{z}; q, t)$ are nonsymmetric variants of Hall-Littlewood polynomials. Given a dominant weight λ , successively applying the operators \mathfrak{T}_i and \mathfrak{L}_i defined in (8) and (10) to \mathbf{z}^λ results in polynomials of this type. The operators \mathfrak{T}_i are used for the results of this paper and [13], while the \mathfrak{L}_i appear in the results of [3]. Given any $w \in W$ and a reduced expression $w = s_{i_1} \cdots s_{i_k}$, set $\mathfrak{T}_w = \mathfrak{T}_{i_1} \cdots \mathfrak{T}_{i_k}$, which is well-defined because the \mathfrak{T}_i satisfy the braid relations. We will similarly write $\mathfrak{L}_w = \mathfrak{L}_{i_1} \cdots \mathfrak{L}_{i_k}$. In this section we will prove a number of results comparing and contrasting the $\mathfrak{T}_w \mathbf{z}^\lambda$ and $\mathfrak{L}_w \mathbf{z}^\lambda$. Since we will obtain a relationship between them in Proposition 8.3, we will first explain how they are different using the affine Hecke algebra.

The affine Hecke algebra $\tilde{\mathcal{H}}_v$ is generated by operators T_i satisfying the braid relations and quadratic relations $T_i^2 = (v-1)T_i + v$, together with a subalgebra θ_Λ isomorphic to the group algebra of the weight lattice Λ , subject to the Bernstein relations

$$(31) \quad \theta_\lambda T_i - T_i \theta_{s_i \lambda} = (v-1) \frac{\theta_\lambda - \theta_{s_i \lambda}}{1 - \theta_{-\alpha_i^\vee}}.$$

We will denote by \mathcal{H}_v the finite Hecke algebra generated by just the T_i . The operators $\mathfrak{T}_{i,v}$ (respectively $\mathfrak{L}_{i,v}$) satisfy the braid and quadratic relations, so they generate algebras of operators on \mathcal{O} isomorphic to \mathcal{H}_v . These representations of \mathcal{H}_v are not irreducible but they may be extended to irreducible representations of $\tilde{\mathcal{H}}_v$ by letting θ_λ act by multiplication by $\mathbf{z}^{-\lambda}$. For the \mathfrak{L}_i , this representation is due to Lusztig [32]; for the \mathfrak{T}_i , see [13].

The two irreducible representations are not isomorphic. This may be seen by noting that the representations are generated by a single \mathcal{H}_v stable vector. For we have

$$(32) \quad \mathfrak{L}_{i,v} \cdot 1 = v, \quad \mathfrak{T}_{i,v} \cdot \mathbf{z}^{-\rho} = -\mathbf{z}^{-\rho}.$$

It is easy to see that there is no $f \in \mathcal{O}$ such that $\mathfrak{L}_{i,v} f = -f$, so these two representations of $\tilde{\mathcal{H}}_v$ are not isomorphic.

A second distinction between the operators \mathfrak{L}_i and \mathfrak{T}_i is given in the following Proposition, which shows how the corresponding spherical idempotents in the Hecke algebra act on a dominant weight: one produces a Schur function times a deformed Weyl denominator; the other produces a (symmetric) Hall-Littlewood polynomial. Define

$$\Theta = \mathbf{z}^{-\rho} \prod_{\alpha \in \Delta^+} (1 - \mathbf{z}^{-\alpha})^{-1} \left(\sum_{w \in W} (-1)^{\ell(w)} w \right) \mathbf{z}^\rho.$$

By the Weyl character formula if λ is a partition then $\Theta \mathbf{z}^\lambda = s_\lambda(\mathbf{z})$ is the Schur function.

Proposition 8.2. *We have*

$$\sum_{w \in W} \mathfrak{T}_w = \left(\prod_{\alpha \in \Delta^+} (1 - v \mathbf{z}^{-\alpha}) \right) \Theta, \quad \sum_{w \in W} \mathfrak{L}_w = \Theta \prod_{\alpha \in \Delta^+} (1 - v \mathbf{z}^{-\alpha}).$$

Proof. The operator (9) of [12] becomes our $\mathfrak{L}_{i,v}$ under the specialization $\pi^\lambda \mapsto \mathbf{z}^{-\lambda}$ and $\epsilon(T_i) = q$, and taking q to be our v . Therefore Theorem 14 of that paper gives both formulas. \square

By (1.1) in Chapter III of Macdonald [33], it follows that if λ is a partition then

$$(33) \quad \sum_{w \in W} \mathfrak{L}_w \mathbf{z}^\lambda = R_\lambda(\mathbf{z}; v) = v_\lambda(v) P_\lambda(\mathbf{z}; v)$$

where R_λ , v_λ and P_λ are as in [33] Section III.1: P_λ is the Hall-Littlewood symmetric polynomial.

Despite the differences between the \mathfrak{L}_i and \mathfrak{T}_i , we have the following relation, where we add v -dependence to the notation for \mathfrak{L}_w and \mathfrak{T}_w .

Proposition 8.3. *For any $w \in W$,*

$$(34) \quad \mathfrak{L}_{w,v} = (-v)^{\ell(w)} \mathbf{z}^\rho \mathfrak{T}_{w,v^{-1}} \mathbf{z}^{-\rho}.$$

Proof. Let $\mathfrak{L}'_{i,v} = -v \mathfrak{L}_{i,v^{-1}}$. Then, using (10),

$$\mathfrak{L}'_{i,v} = (\mathbf{z}^{\alpha_i} - 1)^{-1} (1 - \mathbf{z}^{\alpha_i} s_i) - v (\mathbf{z}^{\alpha_i} - 1)^{-1} (1 - s_i).$$

From this we see that $\mathfrak{L}'_{i,v} = \mathbf{z}^\rho \mathfrak{T}_{i,v} \mathbf{z}^{-\rho}$ which implies (34). \square

Proposition 8.3 gives a relationship between the $\mathfrak{L}_w \mathbf{z}^\lambda$ and $\mathfrak{T}_w \mathbf{z}^\lambda$ for any w . It is only when we sum over all $w \in W$ that the resulting functions appear truly different; the $\mathfrak{L}_w \mathbf{z}^\lambda$ can be assembled into Hall-Littlewood symmetric functions, while the $\mathfrak{T}_w \mathbf{z}^\lambda$ can be assembled into Schur functions multiplied by a deformed Weyl denominator.

We may similarly use Proposition 8.3 and the results of [13] to express either family of functions in terms of nonsymmetric Macdonald polynomials. The notation of Haglund, Haiman and Loehr [21] that we follow here differs from the notation in [13] by the variable change $(q, t) \mapsto (q^{-1}, t^{-1})$, so Theorem 7 of [13] will now be written

$$(35) \quad \phi_w(\mathbf{z}; \varpi^{-\lambda}) = \mathfrak{T}_{w,v}(\mathbf{z}^\lambda) = (-v)^{\ell(w)} \mathbf{z}^{-\rho} w_0 E_{w_0 w(\lambda+\rho)}(\mathbf{z}; \infty, v).$$

The next result is an analog of this for the $\mathfrak{L}_{w,v}$.

Proposition 8.4. *If λ is dominant, then*

$$(36) \quad \mathfrak{L}_{w,v}(\mathbf{z}^{\lambda+\rho}) = w_0 E_{w_0 w(\lambda+\rho)}(\mathbf{z}; \infty, v^{-1}).$$

Proof. This follows by comparing (34) and (35). Another proof may be based on the Knop-Sahi recurrence ([24, 40, 17]) and other facts that can be found in [21]. For brevity we will not give this alternative proof. \square

An implication of this is that there are Whittaker functions whose values are Hall-Littlewood polynomials. These were previously described by Jian-Shu Li [31].

Proposition 8.5. *Let λ be a dominant weight. Then*

$$\mathbf{z}^\rho \sum_w (-v)^{-\ell(w)} \phi_w(\mathbf{z}; \varpi^{-\lambda}) = P_{\lambda+\rho}(\mathbf{z}, v^{-1}).$$

Proof. Multiplying (35) by $\mathbf{z}^\rho (-v)^{-\ell(w)}$ and summing over w , then using (36) and (33), the left-hand side equals

$$\sum_w w_0 E_{w_0 w(\lambda+\rho)}(\mathbf{z}; \infty, v) = \sum_w \mathfrak{L}_{w,v^{-1}}(\mathbf{z}^{\lambda+\rho}) = v_{\lambda+\rho}(v^{-1}) P_{\lambda+\rho}(\mathbf{z}, v^{-1}).$$

Because $\lambda + \rho$ is strongly dominant $v_{\lambda+\rho} = 1$ and the statement follows. \square

Lemma 8.6. *The operator denoted T_i in [3] (5.2.3) or (1.5.5) is the operator $\mathfrak{L}_{i,v}$ conjugated by the map $\mathbf{z} \rightarrow \mathbf{z}^{-1}$. It also equals $\mathfrak{L}_{i,v^{-1}}^{-1}$.*

Proof. This is easily checked. \square

We may now resume the comparison of our models with those in [3] which we addressed in Remark 4.6 and Section 7. Now let us compare $\phi_w(\mathbf{z}; \varpi^{-\lambda})$, where $w_2 = 1$, with the spin $s = 0$ case of the functions f_δ defined in [3]. It follows from Lemma 8.6 that $f_{w\delta}(\mathbf{z}^{-1}) = \mathfrak{L}_w \mathbf{z}^{-\delta}$. Now Proposition 8.3 appears as a relationship between these functions and our $\phi_w(\mathbf{z}; \varpi^{-\lambda})$ with $\delta = -\lambda$. Theorem 7.2 is another statement of such a relationship.

9. INTERTWINING INTEGRALS AND R -MATRICES

In this section, we explore further the dictionary between p -adic representation theory and R -matrices of quantum groups, using lattice models as a pictorial expression of either side. On the representation theory side, facts about standard intertwining operators on unramified principal series were critical to the proofs of Section 2 and in [15]. Roughly speaking, we show that the restrictions of our R -matrix for the quantum superalgebra $U_q(\widehat{\mathfrak{gl}}(r|1))$ to the smaller quantum groups $U_q(\widehat{\mathfrak{gl}}(r))$ and $U_q(\widehat{\mathfrak{gl}}(1))$ neatly express the action of intertwining operators on standard Iwahori fixed vectors (Theorem 9.3) and on Whittaker functionals (Remark 9.5), respectively. To prove Theorem 9.3, we identify the R -matrix for $U_q(\widehat{\mathfrak{gl}}(r))$ and the intertwining integral acting on standard Iwahori fixed vectors with a part of the colored R -matrix in Figure 9. This allows us to give a pictorial interpretation of the functional equations used to prove Proposition 2.4 (see equation (42)).

Before commencing the proofs of these facts, we make several comments related to Theorem 9.3. A common principle in the theory of symmetric functions (related to Schur duality) is to consider the coefficient of $z_1 \cdots z_r$ in the r variables z_i as having some combinatorial significance. Applying this to Schur functions gives the representation degrees of the irreducible representations of the symmetric group, and this principle was also used by Stanley [41] in counting the number of reduced words for the longest element of S_r .

A somewhat analogous procedure (related to Schur-Jimbo duality [23]) is to consider the space of vectors of the form (40) below in a tensor representation of $U_q(\widehat{\mathfrak{gl}}(r))$. These vectors are like the monomials $z_1 \cdots z_r$, because there are no repetitions allowed among the indexing set. The R -matrix acts on these vectors and we will relate this fact to the action of the intertwining operators on the Iwahori fixed vectors.

The larger quantum group $U_q(\widehat{\mathfrak{gl}}(r|1))$ will not appear in Theorem 9.3, only $U_q(\widehat{\mathfrak{gl}}(r))$. Concretely, the reason for this is that \oplus spins do not appear on the right boundary of our systems. We relate the \oplus spins with the Whittaker functional in Remark 9.5.

As in the previous section, q will in this section *not* be the cardinality of the residue field; instead it will here stand for the quantum parameter q in $U_q(\widehat{\mathfrak{gl}}(r))$ as is customary in quantum group theory. We will continue to denote the cardinality of the residue field of F by v^{-1} . With these conventions, we set $q^2 = v$ for Theorem 9.3, consistent with our relation between quantum groups and residue field cardinalities in earlier sections (where we wrote $U_{\sqrt{v}}$).

Consider the quantum loop group $U_q(\widehat{\mathfrak{gl}}(r))$, which is a quantization of a central extension of the loop algebra of $\mathfrak{gl}(r)$; for its formal definition see Section 12.2 in [16]. The quantum loop group acts on the evaluation representation $V_r(z)$ for $z \in \mathbb{C}^\times$. The evaluation representation has a basis $\{v_i(z), 1 \leq i \leq r\}$. Denote $V_r(\mathbf{z}) := V_r(z_1) \otimes \cdots \otimes V_r(z_r)$.

There is an affine R -matrix, initially due to Jimbo [22], that intertwines between tensor products of evaluation representations. We denote it by $R_q(\mathbf{z}^{\alpha_k}) : V_r(z_k) \otimes V_r(z_{k+1}) \rightarrow$

$V_r(z_{k+1}) \otimes V_r(z_k)$. It is given by the following formula:

$$(37) \quad R_q(\mathbf{z}^{\alpha_k}) = \sum_{1 \leq i \leq r} (q - \mathbf{z}^{\alpha_k} q^{-1}) e_{ii} \otimes e_{ii} + \sum_{i > j} (-q^{-1})(1 - \mathbf{z}^{\alpha_k}) e_{ij} \otimes e_{ji} + (-q)(1 - \mathbf{z}^{\alpha_k}) e_{ji} \otimes e_{ij} \\ + \sum_{i > j} (q - q^{-1}) e_{jj} \otimes e_{ii} + \mathbf{z}^{\alpha_k} (q - q^{-1}) e_{ii} \otimes e_{jj}.$$

In the above, e_{ij} stands for the $r \times r$ matrix with a 1 in the (i, j) entry and all other entries equal to 0. It is a map $V_r(z_k) \rightarrow V_r(z_{k+1})$ if it is on the left of the tensor product and $V_r(z_{k+1}) \rightarrow V_r(z_k)$ if it is on the right of the tensor product.

Remark 9.1. This is not exactly the R-matrix in [22]; it is a Drinfeld twist by $-q$. See [6] for a definition of the Drinfeld twist and details on how it modifies an R-matrix. This particular Drinfeld twist appears very often when one deals with $U_q(\widehat{\mathfrak{gl}}(r))$ lattice models. Let us consider the weights in our Figure 23 in which we restrict to configurations with all edges colored. This is the $U_q(\widehat{\mathfrak{gl}}(r))$ portion of the larger $U_q(\widehat{\mathfrak{gl}}(r|1))$ R-matrix. These are the same as the weights in Figure 2.1.8 of [3] (up to a factor, and their q is our q^2). Both R-matrices come from the same Drinfeld twist of $U_q(\widehat{\mathfrak{gl}}(r))$. Throughout this section, when we write $U_q(\widehat{\mathfrak{gl}}(r))$, we will in fact refer to a Drinfeld twist of the usual affine quantum group that produces the R-matrix $R_q(\mathbf{z}^{\alpha_k})$.

It is a standard fact in the theory of quantum groups that $R_q(\mathbf{z}^{\alpha_k})$ is a $U_q(\widehat{\mathfrak{gl}}(r))$ -module homomorphism. We will also denote by $(R_q(\mathbf{z}^{\alpha_k}))_{k,k+1} : V_r(\mathbf{z}) \rightarrow V_r(s_k \mathbf{z})$ the map that acts as $R_q(\mathbf{z}^{\alpha_k})$ on the k and $k+1$ tensor components of $V_r(\mathbf{z})$ and the identity elsewhere.

Consider the R-matrix in Figure 9 restricted to vertices where all edges are colored. It is preferable to normalize the weights of $R(z_{k+1}, z_k)$ by dividing by z_{k+1} so that they may be expressed in terms of $\mathbf{z}^{\alpha_k} = z_k/z_{k+1}$. Denote the resulting restricted R-matrix by $R_{\text{col}}(\mathbf{z}^{\alpha_k})$, and similarly the normalized, restricted version of $R(z_k, z_{k+1})$ is then $R_{\text{col}}(\mathbf{z}^{-\alpha_k})$. The vertices and weights are pictured in Figure 23.

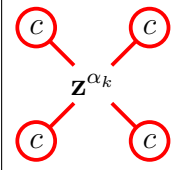
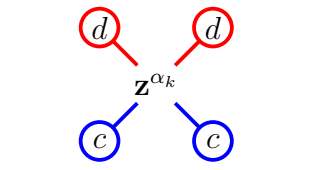
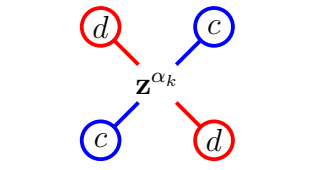
		
$1 - v\mathbf{z}^{\alpha_k}$	$(1 - v)$ if $c < d$ $(1 - v)\mathbf{z}^{\alpha_k}$ if $c > d$	$1 - \mathbf{z}^{\alpha_k}$ if $c > d$ $v(1 - \mathbf{z}^{\alpha_k})$ if $c < d$

FIGURE 23. The colored R-matrix $R_{\text{col}}(\mathbf{z}^{\alpha_k})$. The colors $c, d \in \{1, 2, \dots, r\}$ are always distinct.

Given $w \in S_r$, denote by $w(i)$ the image of the number i under the permutation w . So if $s_1 s_2 \in S_3$, then $s_1 s_2(3) = 1$. In the notation of Section 2, let $\bar{\mathcal{A}}_{s_k}^{\mathbf{z}} := (1 - \mathbf{z}^{\alpha_k}) \mathcal{A}_{s_k}^{\mathbf{z}}$.

Proposition 9.2. Equation (7) can be rewritten as

$$(38) \quad \bar{\mathcal{A}}_{s_k}^{\mathbf{z}}(\Phi_w^{\mathbf{z}}) = \text{wt} \left(\begin{array}{cc} \textcircled{w_{k+1}} & \textcircled{w_{k+1}} \\ & \mathbf{z}^{\alpha_k} \\ \textcircled{w_k} & \textcircled{w_k} \end{array} \right) \Phi_w^{s_k \mathbf{z}} + \text{wt} \left(\begin{array}{cc} \textcircled{w_k} & \textcircled{w_{k+1}} \\ & \mathbf{z}^{\alpha_k} \\ \textcircled{w_{k+1}} & \textcircled{w_k} \end{array} \right) \Phi_{s_k w}^{s_k \mathbf{z}},$$

where w_k stands for $w(k)$ and w_{k+1} stands for $w(k+1)$.

Proof. We shall use the well-known fact that given $s_k, w \in S_r$, then $\ell(s_k w) > \ell(w)$ if and only if $w(k+1) > w(k)$.

Let us do the proof for when $\ell(s_k w) > \ell(w)$, the opposite case is similar. Our assumption implies that $w(k+1) > w(k)$. By consulting the weights in Figure 23, we see that

$$\text{wt} \left(\begin{array}{cc} \textcircled{w_{k+1}} & \textcircled{w_{k+1}} \\ & \mathbf{z}^{\alpha_k} \\ \textcircled{w_k} & \textcircled{w_k} \end{array} \right) = 1 - v, \quad \text{wt} \left(\begin{array}{cc} \textcircled{w_k} & \textcircled{w_{k+1}} \\ & \mathbf{z}^{\alpha_k} \\ \textcircled{w_{k+1}} & \textcircled{w_k} \end{array} \right) = 1 - \mathbf{z}^{\alpha_k}.$$

and the equivalence follows immediately by comparison with equation (7). \square

We remind the reader that the colors indexing edges in the R-matrix $R_{\text{col}}(\mathbf{z}^{\alpha_k})$ are denoted by $\{1, \dots, r\}$. We can then think of the R-matrix $R_{\text{col}}(\mathbf{z}^{\alpha_k})$ as a map $R_{\text{col}}(\mathbf{z}^{\alpha_k}) : U_r(z_k) \otimes U_r(z_{k+1}) \rightarrow U_r(z_{k+1}) \otimes U_r(z_k)$, where $U_r(z)$ is a vector space with formal basis elements $u_i(z)$ associated to the colors i for $1 \leq i \leq r$. One can write the R-matrix in Figure 23 in matrix form as follows:

$$(39) \quad R_{\text{col}}(\mathbf{z}^{\alpha_k}) = \sum_{1 \leq i \leq r} \text{wt} \left(\begin{array}{cc} \textcircled{i} & \textcircled{i} \\ & \mathbf{z}^{\alpha_k} \\ \textcircled{i} & \textcircled{i} \end{array} \right) e_{ii} \otimes e_{ii} + \sum_{i > j} \text{wt} \left(\begin{array}{cc} \textcircled{j} & \textcircled{i} \\ & \mathbf{z}^{\alpha_k} \\ \textcircled{i} & \textcircled{j} \end{array} \right) e_{ij} \otimes e_{ji} \\ + \text{wt} \left(\begin{array}{cc} \textcircled{i} & \textcircled{j} \\ & \mathbf{z}^{\alpha_k} \\ \textcircled{j} & \textcircled{i} \end{array} \right) e_{ji} \otimes e_{ij} + \sum_{i > j} \text{wt} \left(\begin{array}{cc} \textcircled{i} & \textcircled{i} \\ & \mathbf{z}^{\alpha_k} \\ \textcircled{j} & \textcircled{j} \end{array} \right) e_{jj} \otimes e_{ii} + \text{wt} \left(\begin{array}{cc} \textcircled{j} & \textcircled{j} \\ & \mathbf{z}^{\alpha_k} \\ \textcircled{i} & \textcircled{i} \end{array} \right) e_{ii} \otimes e_{jj}.$$

Having expressed the matrix $R_{\text{col}}(\mathbf{z}^{\alpha_k})$ in this way, it is now simple to compare it to $-qR_q(\mathbf{z}^{\alpha_k})$ in (37) with $v = q^2$. All but the coefficients of $e_{ii} \otimes e_{ii}$ are seen to match, which will be an important ingredient in our next theorem.

Let \mathbb{I} be the set of elements in $\{1, \dots, r\}^r$ that have no repeated entries and let $\mathbf{i}_0 := (1, 2, \dots, r) \in \mathbb{I}$. It is easy to show that the set \mathbb{I} is in bijection with the set $\{w(\mathbf{i}_0), w \in S_r\}$, where S_r acts on elements in \mathbb{I} by permuting the entries. Note that the action of S_r on \mathbb{I} is regular, i.e. transitive and free.

For $\mathbf{i} = (i_1, \dots, i_r) \in \mathbb{I}$, define

$$(40) \quad v_{\mathbf{i}}(\mathbf{z}) := v_{i_1}(z_1) \otimes \dots \otimes v_{i_r}(z_r) \in V_r(\mathbf{z}).$$

Denote by $V_r^{\text{alt}}(\mathbf{z})$ the subspace of $V_r(\mathbf{z})$ with basis $\{v_{\mathbf{i}}(\mathbf{z}), \mathbf{i} \in \mathbb{I}\}$. Note that this is *not* a $U_q(\widehat{\mathfrak{gl}}(r))$ submodule of $V_r(\mathbf{z})$. Consider the following isomorphism of vector spaces $\Psi_{\mathbf{z}} :$

$I(\mathbf{z})^J \rightarrow V_r^{\text{alt}}(\mathbf{z})$ defined as:

$$(41) \quad \Psi_{\mathbf{z}}(\Phi_w^{\mathbf{z}}) := v_{w(\mathbf{i}_0)}(\mathbf{z}).$$

Theorem 9.3. *The following diagram commutes assuming $v = q^2$.*

$$\begin{array}{ccc} I(\mathbf{z})^J & \xrightarrow{\Psi_{\mathbf{z}}} & V_r^{\text{alt}}(\mathbf{z}) \\ \downarrow \bar{\mathcal{A}}_{s_k}^{\mathbf{z}} & & \downarrow (-qR_q(\mathbf{z}^{\alpha_k}))_{k,k+1} \\ I(s_k \mathbf{z})^J & \xrightarrow{\Psi_{s_k \mathbf{z}}} & V_r^{\text{alt}}(s_k \mathbf{z}) \end{array}$$

Proof. By Proposition 9.2, we only have to match all the entries of the R-matrices in equations (37) and (39) *except* the first entry (the entry colored with red only in equation (39) does not appear in the intertwining integral (38)). As noted above, the matching is simple to do: for example the last entry in equation (39) has weight $(1-v)\mathbf{z}^{\alpha_k}$, while the last entry in equation (37) multiplied by $-q$ has weight $(1-q^2)\mathbf{z}^{\alpha_k}$. \square

Remark 9.4. The theorem above can also be proven if we set $q^2 = v^{-1}$ (as opposed to $q^2 = v$). In that setting the quantum group needs to be Drinfeld twisted by q^{-1} (as opposed to by $(-q)$). We made this choice to be in agreement with [5, Theorem 1], but both choices might be useful when considering representation theoretic applications of this result.

Remark 9.5. Note that Proposition 2.3 can be rewritten as

$$\Omega_{s_i \mathbf{z}} \circ \bar{\mathcal{A}}_{s_i}^{\mathbf{z}} = (1 - v\mathbf{z}^{-\alpha_i})\Omega_{\mathbf{z}}.$$

The factor $1 - v\mathbf{z}^{-\alpha_i}$ agrees up to a scalar with the fully uncolored Boltzmann weight for $R(z_{i+1}, z_i)$ in Figure 9 and should be thought of as the R-matrix for the evaluation module of $U_q(\widehat{\mathfrak{gl}}(1)) \subset U_q(\widehat{\mathfrak{gl}}(r|1))$.

We now give a pictorial interpretation of the functional equations used to prove Proposition 2.4 for values of Iwahori Whittaker functions and partition functions. The way to prove such functional equations for Iwahori Whittaker functions is to compute the expression $\Omega_{s_i \mathbf{z}}(\pi(\varpi^{-\lambda} w_2) \bar{\mathcal{A}}_{s_i}^{\mathbf{z}} \Phi_{w_1}^{\mathbf{z}})$ for a given (λ, w_1, w_2) in two different ways using results of Casselman and Shalika (written earlier as equation (5) and Proposition 2.3). This can be represented as follows, remembering the shift by \mathbf{z}^ρ to relate Whittaker functions to lattice model partition functions in Theorem 5.2 which accounts for the factor of $\mathbf{z}^{-\alpha_i}$ in the first quantity below:

$$\begin{aligned} & \text{wt} \left(\begin{array}{cc} \textcircled{+} & \textcircled{+} \\ \textcircled{+} & \textcircled{+} \end{array} \right)_{\mathbf{z}^{\alpha_i}} \mathbf{z}^{-\alpha_i} \Omega_{\mathbf{z}}(\pi(\varpi^{-\lambda} w_2) \Phi_{w_1}^{\mathbf{z}}) = (1 - v\mathbf{z}^{-\alpha_i}) \Omega_{\mathbf{z}}(\pi(\varpi^{-\lambda} w_2) \Phi_{w_1}^{\mathbf{z}}) \\ (42) \quad & = \Omega_{s_i \mathbf{z}} \circ \bar{\mathcal{A}}_{s_i}^{\mathbf{z}}(\pi(\varpi^{-\lambda} w_2) \Phi_{w_1}^{\mathbf{z}}) = \Omega_{s_i \mathbf{z}}(\pi(\varpi^{-\lambda} w_2) \bar{\mathcal{A}}_{s_i}^{\mathbf{z}} \Phi_{w_1}^{\mathbf{z}}) \\ & = \text{wt} \left(\begin{array}{cc} \textcircled{w_{i+1}} & \textcircled{w_{i+1}} \\ \textcircled{w_i} & \textcircled{w_i} \end{array} \right)_{\mathbf{z}^{\alpha_i}} \Omega_{s_i \mathbf{z}}(\pi(\varpi^{-\lambda} w_2) \Phi_{w_1}^{s_i \mathbf{z}}) + \text{wt} \left(\begin{array}{cc} \textcircled{w_i} & \textcircled{w_{i+1}} \\ \textcircled{w_{i+1}} & \textcircled{w_i} \end{array} \right)_{\mathbf{z}^{\alpha_i}} \Omega_{s_i \mathbf{z}}(\pi(\varpi^{-\lambda} w_2) \Phi_{w_1}^{s_i \mathbf{z}}). \end{aligned}$$

As the first equality (from Remark 9.5) and the last equality (from Proposition 9.2) demonstrate, the uncolored and all-colored R-vertices neatly express these two ways of

evaluating the expression on the middle line above. The effect of the intertwining integral on the space of Whittaker functionals is the same as the effect of the uncolored R-matrix on the left boundary of the lattice model, while the effect of the intertwining integral on the space of Iwahori fixed vectors is the same as the effect of the colored R-matrix on the right boundary of the lattice model. The equality of the first and last quantities in the string of equalities above may be proved via solvable lattice models using the familiar train argument as depicted in Figure 18.

This phenomena also appears in the theory of metaplectic spherical Whittaker functions for an n -fold metaplectic cover of $\mathrm{GL}_r(F)$, which can also be realized as partition functions of a solvable lattice model. In that case the action of the intertwining integral on the space of Whittaker functionals is the Kazhdan-Patterson scattering matrix, which has been interpreted (up to a Drinfeld twist) as the $U_q(\widehat{\mathfrak{gl}}(n))$ R-matrix in [5, Theorem 1], while the action of the intertwining integral on the spherical vector is a factor which can be interpreted as the spin \oplus part of a larger R-matrix. The train argument for the associated lattice models involves exactly these R-matrices. This seems like a compelling connection between two a priori different methods of argument, and we hope it will be useful in further relating the representation theories of p -adic and quantum groups.

REFERENCES

- [1] Rodney J. Baxter. *Exactly solved models in statistical mechanics*. Academic Press Inc. [Harcourt Brace Jovanovich Publishers], London, 1982.
- [2] Alexei Borodin, Alexey Bufetov, and Michael Wheeler. Between the stochastic six vertex model and Hall-Littlewood processes, 2016, arXiv:1611.09486.
- [3] Alexei Borodin and Michael Wheeler. Coloured stochastic vertex models and their spectral theory, 2018, arXiv:1808.01866.
- [4] Alexei Borodin and Michael Wheeler. Nonsymmetric Macdonald polynomials via integrable vertex models, 2019, arXiv:1904.06804.
- [5] Ben Brubaker, Valentin Buciumas, and Daniel Bump. A Yang-Baxter equation for metaplectic ice. *Commun. Number Theory Phys.*, 13(1):101–148, 2019.
- [6] Ben Brubaker, Valentin Buciumas, Daniel Bump, and Solomon Friedberg. Hecke modules from metaplectic ice. *Selecta Math. (N.S.)*, 24(3):2523–2570, 2018.
- [7] Ben Brubaker, Valentin Buciumas, Daniel Bump, and Henrik Gustafsson. Vertex operators, solvable lattice models and metaplectic Whittaker functions, 2018, arXiv:1806.07776.
- [8] Ben Brubaker, Valentin Buciumas, Daniel Bump, and Henrik P. A. Gustafsson. Colored five-vertex models and Demazure atoms, 2019, arXiv:1902.01795.
- [9] Ben Brubaker, Daniel Bump, Gautam Chinta, Solomon Friedberg, and Paul E. Gunnells. Metaplectic ice. In *Multiple Dirichlet series, L-functions and automorphic forms*, volume 300 of *Progr. Math.*, pages 65–92. Birkhäuser/Springer, New York, 2012.
- [10] Ben Brubaker, Daniel Bump, and Solomon Friedberg. Schur polynomials and the Yang-Baxter equation. *Comm. Math. Phys.*, 308(2):281–301, 2011.
- [11] Ben Brubaker, Daniel Bump, and Solomon Friedberg. *Weyl group multiple Dirichlet series: type A combinatorial theory*, volume 175 of *Annals of Mathematics Studies*. Princeton University Press, Princeton, NJ, 2011.
- [12] Ben Brubaker, Daniel Bump, and Solomon Friedberg. Matrix coefficients and Iwahori-Hecke algebra modules. *Adv. Math.*, 299:247–271, 2016.
- [13] Ben Brubaker, Daniel Bump, and Anthony Licata. Whittaker functions and Demazure operators. *J. Number Theory*, 146:41–68, 2015.
- [14] W. Casselman. The unramified principal series of p -adic groups. I. The spherical function. *Compositio Math.*, 40(3):387–406, 1980.

- [15] W. Casselman and J. Shalika. The unramified principal series of p -adic groups. II. The Whittaker function. *Compositio Math.*, 41(2):207–231, 1980.
- [16] Vyjayanthi Chari and Andrew Pressley. *A guide to quantum groups*. Cambridge University Press, Cambridge, 1994.
- [17] Ivan Cherednik. Intertwining operators of double affine Hecke algebras. *Selecta Math. (N.S.)*, 3(4):459–495, 1997.
- [18] Gautam Chinta, Paul E. Gunnells, and Anna Puskás. Metaplectic Demazure operators and Whittaker functions. *Indiana Univ. Math. J.*, 66(3):1045–1064, 2017, arXiv:1408.5394.
- [19] Sergey Fomin and Anatol N. Kirillov. The Yang-Baxter equation, symmetric functions, and Schubert polynomials. In *Proceedings of the 5th Conference on Formal Power Series and Algebraic Combinatorics (Florence, 1993)*, volume 153, pages 123–143, 1996.
- [20] Nathan Gray. Metaplectic ice for Cartan type C, 2017, arXiv:1709.04971.
- [21] J. Haglund, M. Haiman, and N. Loehr. A combinatorial formula for Macdonald polynomials. *J. Amer. Math. Soc.*, 18(3):735–761, 2005.
- [22] Michio Jimbo. A q -difference analogue of $U(\mathfrak{g})$ and the Yang-Baxter equation. *Lett. Math. Phys.*, 10(1):63–69, 1985.
- [23] Michio Jimbo. A q -analogue of $U(\mathfrak{gl}(N+1))$, Hecke algebra, and the Yang-Baxter equation. *Lett. Math. Phys.*, 11(3):247–252, 1986.
- [24] Friedrich Knop. Integrality of two variable Kostka functions. *J. Reine Angew. Math.*, 482:177–189, 1997.
- [25] Allen Knutson and Paul Zinn-Justin. Schubert puzzles and integrability I: invariant trilinear forms, 2017, arXiv:1706.10019.
- [26] Takeo Kojima. Diagonalization of transfer matrix of supersymmetry $U_q(\widehat{\mathfrak{sl}}(M+1|N+1))$ chain with a boundary. *J. Math. Phys.*, 54(4):043507, 40, 2013.
- [27] Christian Korff. Cylindric versions of specialised Macdonald functions and a deformed Verlinde algebra. *Comm. Math. Phys.*, 318(1):173–246, 2013.
- [28] P. P. Kulish, N. Yu. Reshetikhin, and E. K. Sklyanin. Yang-Baxter equations and representation theory. I. *Lett. Math. Phys.*, 5(5):393–403, 1981.
- [29] Greg Kuperberg. Another proof of the alternating-sign matrix conjecture. *Internat. Math. Res. Notices*, (3):139–150, 1996.
- [30] Alain Lascoux, Bernard Leclerc, and Jean-Yves Thibon. Flag varieties and the Yang-Baxter equation. *Lett. Math. Phys.*, 40(1):75–90, 1997.
- [31] Jian-Shu Li. Some results on the unramified principal series of p -adic groups. *Math. Ann.*, 292(4):747–761, 1992.
- [32] George Lusztig. Equivariant K -theory and representations of Hecke algebras. *Proc. Amer. Math. Soc.*, 94(2):337–342, 1985.
- [33] I. Macdonald. *Symmetric Functions and Hall Polynomials*. Oxford Mathematical Monographs. The Clarendon Press Oxford University Press, New York, second edition, 1995. With contributions by A. Zelevinsky, Oxford Science Publications.
- [34] Jun Murakami. The free-fermion model in presense [presence] of field related to the quantum group $\mathcal{U}_q(\widehat{\mathfrak{sl}}_2)$ of affine type and the multi-variable Alexander polynomial of links. In *Infinite analysis, Part A, B (Kyoto, 1991)*, volume 16 of *Adv. Ser. Math. Phys.*, pages 765–772. World Sci. Publ., River Edge, NJ, 1992.
- [35] Manish Patnaik and Anna Puskás. On Iwahori-Whittaker functions for metaplectic groups. *Adv. Math.*, 313:875–914, 2017.
- [36] Jacques H. H. Perk and Cherie L. Schultz. New families of commuting transfer matrices in q -state vertex models. *Phys. Lett. A*, 84(8):407–410, 1981.
- [37] L. Poulain d’Andecy. Fusion formulas and fusion procedure for the Yang-Baxter equation. *Algebr. Represent. Theory*, 20(6):1379–1414, 2017, arXiv:1307.6808.
- [38] Mark Reeder. p -adic Whittaker functions and vector bundles on flag manifolds. *Compositio Math.*, 85(1):9–36, 1993.
- [39] François Rodier. Modèle de Whittaker des représentations admissibles des groupes réductifs p -adiques déployés. *C. R. Acad. Sci. Paris Sér. A-B*, 275:A1045–A1048, 1972.

- [40] Siddhartha Sahi. Interpolation, integrality, and a generalization of Macdonald's polynomials. *Internat. Math. Res. Notices*, (10):457–471, 1996.
- [41] Richard P. Stanley. On the number of reduced decompositions of elements of Coxeter groups. *European J. Combin.*, 5(4):359–372, 1984.
- [42] Takeshi Tokuyama. A generating function of strict Gelfand patterns and some formulas on characters of general linear groups. *J. Math. Soc. Japan*, 40(4):671–685, 1988.
- [43] Michael Wheeler and Paul Zinn-Justin. Refined Cauchy/Littlewood identities and six-vertex model partition functions: III. Deformed bosons. *Adv. Math.*, 299:543–600, 2016.
- [44] Michael Wheeler and Paul Zinn-Justin. Littlewood-Richardson coefficients for Grothendieck polynomials from integrability. *J. Reine Angew. Math.*, to appear.
- [45] Hiroyuki Yamane. Quantized enveloping algebras associated with simple Lie superalgebras and their universal R -matrices. *Publ. Res. Inst. Math. Sci.*, 30(1):15–87, 1994.

SCHOOL OF MATHEMATICS, UNIVERSITY OF MINNESOTA, MINNEAPOLIS, MN 55455
E-mail address: brubaker@math.umn.edu

SCHOOL OF MATHEMATICS AND PHYSICS, THE UNIVERSITY OF QUEENSLAND, ST. LUCIA, QLD, 4072,
 AUSTRALIA
E-mail address: valentin.buciumas@gmail.com

DEPARTMENT OF MATHEMATICS, STANFORD UNIVERSITY, STANFORD, CA 94305-2125
E-mail address: bump@math.stanford.edu

DEPARTMENT OF MATHEMATICS, STANFORD UNIVERSITY, STANFORD, CA 94305-2125
E-mail address: gustafsson@stanford.edu